f-MOPSO/Div: an improved extreme-point-based multi-objective PSO algorithm applied to a socio-economic-environmental conjunctive water use problem

Farshad Rezaei · Hamid R. Safavi

Abstract In this paper, a new version of the multi-objective particle swarm optimizer named the Diversity-enhanced fuzzy multi-objective particle swarm optimization (f-MOPSO/Div) algorithm is proposed. This algorithm is an improved version of our recently proposed f-MOPSO. In the proposed algorithm, a new characteristic of the particles in the objective space, which we named the "extremity," is also evaluated, along with the Pareto dominance, to appoint proper guides for the particles in the search space. Three improvements are applied to the f-MOPSO to mitigate its shortcomings, generating f-MOPSO/Div: (1) selecting the global best solution based on the diversity of the extreme solutions, (2) impeding the particles to be trapped in the local optima using a mutation scheme based on the dynamic probability, and (3) removing the pre-optimization process. To validate f-MOPSO/Div, it was compared with some other popular multi-objective algorithms on 14 standard low- and high-dimensional test problem suites. After the comparative results indicated the outperformance of the proposal, the f-MOPSO/Div was applied to solve an optimal conjunctive water use management problem, in a semi-arid study area in west-central Iran, over a 13-year long-term planning period with two main objectives: (1) maximizing the aquifer sustainability as an environmental goal, and (2) maximizing the crop yields as a socio-economic goal. As the results suggest, the cumulative groundwater level drawdown is considerably decreased over the whole planning period to make the aquifer sustainable, while the water productivity is held at a desirable level, demonstrating the superiority of the f-MOPSO/Div when also applied to solve a large-scale real-world optimization problem.

Introduction

Multi-objective optimization

In multi-objective optimization, a set of non-dominated solutions is constructed at each iteration and is usually added to an external archive to provide information for selecting the guides. Discriminating the non-dominated solutions from a large set of solutions contributes the promising regions to be found in the search space when the Pareto dominance relation is strong enough to introduce a sufficient number of solutions. In this case, the selection pressure is insufficient; thus, employing some other techniques is required to enable the guides to be designated from the stored non-dominated points. In contrast, the selection of solutions may lead to very poor

F. Rezaei · H. R. Safavi (✉)
Department of Civil Engineering, Isfahan University of Technology, Isfahan, Iran
e-mail: hasafavi@iut.ac.ir

F. Rezaei
e-mail: f.rezaei@alumni.iut.ac.ir

performance when there are weak dominance relations; i.e., a few points are to be discriminated based on the Pareto dominance. In this case, the selection pressure needs to be decreased to allow some dominated solutions to take part in the comparisons for the guide selections. Accordingly, the number of candidate solutions needs to be increased to make the archive diversified enough to cover a large domain of the objective space. Some of the guide selection techniques proposed in the multi-objective algorithms are listed as follows.

1. Randomized selection: This assigns a random number to each non-dominated solution that is found in the optimization process and then selects one of the several solutions taking part in a tournament based on the roulette wheel selection method. The practical applications have proven that this mechanism has poor performance due to the excessive stochastic nature of the selection process (Agrawal et al. 2008)
2. Relaxed Pareto-based dominance methods including ε-dominance (Laumanns et al. 2002), r-dominance (Ben Said et al. 2010), and the grid-based approach (Yang et al. 2013; Liu et al. 2018)
3. Reference point–based dominance techniques (Thiele et al. 2009; Goulart and Campelo 2016; Liu et al. 2017; Wang et al. 2017). In these techniques, all of the results rely on the reference points, and the initial solutions should be diversified enough in the objective space to cover all reference points (Lin et al. 2015).
4. Non-Pareto dominance methods including the maximum fitness (Balling and Wilson 2001), relation favor (RF) (Drechsler et al. 2001), and global detriment (GD) (Garza-Fabre et al. 2009).

Multi-objective particle swarm optimization

The particle swarm optimization (PSO) algorithm, first proposed by Kennedy and Eberhart (1995), is the most commonly used stochastic population-based swarm intelligence technique inspired by the evolution of nature. Compared to other meta-heuristic techniques (e.g., the genetic algorithm), PSO has a more flexible and well-balanced mechanism that can enhance and adapt the global and local exploration, and it needs fewer particles (solutions) to provide the required diversity and a faster convergence rate (Abido 2010). The details of some studies that have addressed the applications of the four

techniques mentioned in the previous subsection for multi-objective PSO (MOPSO) algorithms are summarized in Table 1.

Multi-objective conjunctive water use optimization models

This paper is focused on applying a new MOPSO algorithm to solve a real-world optimal conjunctive water use problem. The conjunctive water use concept was first introduced by Burt (1964). Both sources of surface and groundwater present some desired characteristics. Lack of water losses due to seepage, leakage, evaporation, and water transfer makes groundwater dominate the surface water. Moreover, the large surface water reservoir construction is always challenging environmental problems, adaptation with the society, and economic efficiency (Afshar et al. 2010). The groundwater is never subject to sedimentation and has a low potential for pollution and climate change–related droughts. The main disadvantage of the groundwater resources might be its need for a high amount of energy for pumping from the underlain water table, leading to pay much more costs compared to surface water resources. The surface water benefits from some utilities discriminating it from groundwater, which mainly includes the capability for generating electrical energy by hydropower plants and its application in recreational affairs and flood control. The conjunctive use of both surface and groundwater use can hold a good balance between the advantages and disadvantages of these water resources by increasing the benefits and decreasing the shortcomings of both of them (Hollander et al. 2009). In addition to quantitative benefits conjunctive water use presents, this kind of water use may also improve the water quality by conjunctively salt water–fresh water use, which has a wide effect on increasing water productivity and decreasing the need for desalinization as well as water-logging control. The qualitative water problems are more reported in coastal areas with a high potential of seawater intrusion, which can be handled by conjunctive water use (Yadav et al. 2004; Kaur et al. 2007). Furthermore, in arid and semi-arid regions challenging with population increase, growing agriculture, and developing industries, all of the water quality-quantity problems are more crucial, necessitating conjunctive water use as a solution. In these regions, the climate change impacts are threats to water resources sustainability, provoking water resources management in all its forms, including supply management, demand management,

Table 1 Advantages and disadvantages of several MOPSO algorithms presented in the literature

Authors	Algorithm	Advantages	Disadvantages
Mostaghim and Teich (2003a)	Sigma method	• Assigning each particle a particular global best whose Sigma vector has the smallest distance to that of the certain particle • Speeding up the convergence	• Lacking sufficient diversity • Facing the premature convergence
Mostaghim and Teich (2003b)	ε-dominance	• Restricting the number of non-dominated particles in the external archive • Speeding up the convergence	• Losing diversity • Facing the premature convergence
Ireland et al. (2006)	Centroid method	• Distance-weighted averaging of the archive non-dominated points to calculate a particular guide • Maintaining diversity	• Reducing the convergence rate • Facing the premature convergence
Yang et al. (2009a)		• Combining the Sigma method with the local density around each particle to mitigate the effect of the high convergence speed • Holding a desired balance between the convergence and diversity	
Sahoo et al. (2011)	HSG-MOPSO	• Some specifically chosen dominated solutions are added to the normal non-dominated archive of the MOPSO to keep the diversity • The population members follow their respective nearest guides	• Retarding the convergence • Facing a mild premature convergence
Li et al. (2017)	MOPSO/GMR	• Presenting a novel ranking strategy called the Global Margin Ranking (GMR) to guide the individuals to the margins of the objective space • Combining GMR with the individuals' density	
Rezaei et al. (2017a)	f-MOPSO	• Replacing the diversity criterion with a newly identified criterion called "extremity" • Selecting the guide particles based on dominance and extremity	• The possibility of premature convergence if the particles are engaged in a drift when moving to the extreme points • Needing a pre-optimization process
Nebro et al. (2018)	SMPSO/RP	• Removing the diversified particles located far from the Pareto solutions in favor of returning the nearer ones to the archive • Accelerating the convergence	
Qu et al. (2020)	SS-MOPSO	• Proposing self-organized speciation based MOPSO to solve multi-modal problems • Preserving the diversity through incorporating the non-dominated sorting to a crowding distance sorting mechanism	
The current proposal	f-MOPSO/Div	• Involving the diversity to choose the guides • The desired performance when taking the triple extremity-diversity-dominance criteria • Incorporating a dynamically parameter tuned mutation scheme to avoid local optima • Removing the pre-optimization process	

and supply-demand management in these regions (Safavi et al. 2010).

There is a voluminous literature carried out on the multi-objective optimization of conjunctive surface-ground water use, considering different aspects of management purposes. McPhee and Yeh (2004) developed a decision support system through performing a three-objective optimization method aimed to minimize groundwater level drawdowns and an ε-constraint method to tackle the multi-objective nature of their problem. Yang et al. (2009b) introduced a multi-objective management model utilizing a coupled genetic algorithm-constrained differential dynamic programming method to maximize net agricultural benefits considering constant and variable costs in agricultural activities. Peralta et al. (2014) proposed a simulation-optimization model for optimal conjunctive use of the reservoir-surface-groundwater system. The goals were to maximize water supply and hydropower

generation as well as to minimize surface water transfer and groundwater pumping costs. Srivastava and Singh (2017) employed a fuzzy multi-objective goal programming technique to optimize cropping patterns in a canal command area, regarding several qualitative and quantitative purposes. Sun et al. (2017) utilized a multi-objective model to optimize the cropping pattern in a study area located in the southwest of China. The main goals of the optimization were to maximize the net benefit and to minimize the agricultural drought severity for the main crops as well as the shortages in meeting the irrigation demands supplied by surface water resources to decrease groundwater extraction in the region. Yousefi et al. (2018) conducted a multi-objective conjunctive-treated wastewater and groundwater use management to achieve three main goals: maximizing net benefit, minimizing nitrogen leaching, and maximizing groundwater recharge. They applied two techniques, including single-objective particle swarm optimization (PSO) with an additive weighting method as well as the multi-objective PSO (MOPSO) to solve their multi-objective optimization model. Zeinali et al. (2020) linked a non-dominated sorting genetic algorithm II (NSGA-II) with a coupled WEAP-MODFLOW simulation model targeting (1) maximization of the water demands met and (2) minimization of the cumulative groundwater withdrawal at an operational period in a low-flow area.

The MOPSO algorithm has also been widely used in several water resources management schemes such as reservoir operation, rainfall-runoff modeling, water quality modeling, and groundwater modeling (Jahandideh-Tehrani et al. 2020). Furthermore, as an alternative to conjunctively surface and ground water use, Tayebikhorami et al. (2019) attempted to use the treated wastewater as an unconventional source of water to supply the water demands. They utilized a fuzzy NSGA-II algorithm as the optimizer in which the fuzzy transformation method (FTM) was used to address the potential uncertainties of the system contributing to developing different fuzzy scenarios to account for the uncertainties of the system. Then, the fuzzy parameters confidence levels were included in the optimization sector to facilitate the trade-off curves between the objectives to be generated.

The present work

In this paper, we design and propose an improved version of the multi-objective particle swarm optimization (MOPSO) named f-MOPSO/Div. It is based on the recently proposed f-MOPSO algorithm, which was first proposed in a bi-objective version by Rezaei et al. (2017a) and then in a tri-objective version by Rezaei et al. (2017b). This algorithm uses a Sugeno fuzzy inference system to delineate an index named the comprehensive Dominance Index (DI). This index can evaluate the solutions found at each iteration of the algorithm in terms of both the dominance and "extremity." The extremity, expressing how close a solution is to any of the axes in the objective space, is a previously unidentified characteristic of the solutions in the objective space we found out in this research. In f-MOPSO/Div, the extremity remains as the basis for selecting the personal best particles; however, the "extremity" is replaced by "diversity" as the measure that helps select the global best solution. In this paper, the f-MOPSO/Div is applied to solve a socio-economic-environmental conjunctive water use management problem.

In the remainder of this paper, we first introduce the particle swarm optimization algorithm in detail in "Particle swarm optimization" section. In "Fuzzy-based multi-objective particle swarm optimization" section, we introduce and emphasize the unique capabilities of the f-MOPSO algorithm. In "Proposed diversity-enhanced fuzzy multi-objective PSO" section, we put forward our proposed algorithm (f-MOPSO/Div) consisting of three subsections. "Experimental results on standard benchmark functions" section presents the experimental results of applying the proposed algorithm on a variety of standard benchmark functions. "Conjunctive surface-ground water use management" section introduces the study area and presents the simulation-optimization model's mathematical formulation. "Results and discussion (f-MOPSO/Div application)" section gives results and provides some discussions on them. Finally, "Conclusion" section concludes the paper.

Methodology

Particle swarm optimization

Suppose for a D-dimensional optimization problem that $X_i = (x_{i1}, x_{i2}, \ldots, x_{iD})$ and $V_i = (v_{i1}, v_{i2}, \ldots, v_{iD})$ are the ith particle's position vector and velocity vector, respectively. Assume that $Pbest_i^t = (p_{i1}, p_{i2}, \ldots, p_{iD})$ is the personal best (Pbest) position of the ith particle and $Gbest^t = (p_{g1}, p_{g2}, \ldots, p_{gD})$ represents the global best

(*Gbest*) position of the swarm, where $i \in \{1, 2, \ldots, N\}$, D is the number of dimensions, and N is the swarm size. The velocity and position of each particle is updated using Eqs. (1) and (2):

$$V_i^{t+1} = wV_i^t + c_1r_1\left(Pbest_i^t - X_i^t\right)$$
$$+ c_2r_2\left(Gbest^t - X_i^t\right) \tag{1}$$

$$X_i^{t+1} = X_i^t + V_i^{t+1} \tag{2}$$

where superscript t is the iteration number; w is the inertia weight; r_1 and r_2 are two random vectors; and c_1 and c_2 are the cognitive and social scaling parameters, respectively. An efficient form of Eq. (1) is the constriction coefficient model that is shown below (Rezaei et al. 2017a).

$$V_i^{t+1} = \chi\left[V_i^t + \varphi_1\left(Pbest_i^t - X_i^t\right) + \varphi_2\left(Gbest^t - X_i^t\right)\right] \tag{3}$$

$$\chi = \frac{2k}{\left|2 - \varphi - \sqrt{\varphi(\varphi - 4)}\right|}; \varphi = \varphi_1 + \varphi_2; \varphi_1$$
$$= c_1r_1; \varphi_2 = c_2r_2 \tag{4}$$

where χ is the constriction factor. The parameter $k \in [0, 1]$ in Eq. (4) controls the exploration and exploitation abilities of the swarm, where $k = 1$ denotes full exploration and $k = 0$ suggests full exploitation; however, a transition between $k = 1$ and $k = 0$ could provide a good balance between exploration and exploitation. Hence, k can be calculated as follows:

$$k = k_{max} - \frac{k_{max} - k_{min}}{iter_{max}} \times iter \tag{5}$$

where k_{max} and k_{min} are constants that must be set properly, *iter* is the number of iterations, and $iter_{max}$ is the maximum number of iterations.

Fuzzy-based multi-objective particle swarm optimization

The method was first proposed by Rezaei et al. (2017a). This algorithm helps the MOPSO algorithm select the suitable *Pbests* and *Gbest* for the swarm at each iteration. The algorithm takes advantage of a Sugeno fuzzy inference system (SFIS) to assign an index to each solution to discriminate the best solutions of a population. In f-MOPSO, the SFIS consists of several rules, each of which represents an aggregated membership degree coming from combining the fuzzy membership function values of the objectives as the premises. The SFIS also includes the weighted sum of the objectives as the consequence of each rule. The SFIS rules' consequences represent the partial dominance of the solutions, while the resulting fuzzy membership degree (MD) acts as a weight that is assigned to the partial dominance to stress it. The structure of the SFIS for a multi-/many-objective minimization problem is as follows:

If Z_1' is A_1^1 and Z_2' is A_2^1 and...and Z_M' is A_M^1 Then Z^1
$$= W_1^1Z_1' + W_2^1Z_2' + \ldots + W_M^1Z_M' \tag{6}$$

If Z_1' is A_1^2 and Z_2' is A_2^2 and...and Z_M' is A_M^2 Then Z^2
$$= W_1^2Z_1' + W_2^2Z_2' + \ldots + W_M^2Z_M' \tag{7}$$

$\vdots$

If Z_1' is A_1^N and Z_2' is A_2^N and...and Z_M' is A_M^N Then $Z^N = W_1^NZ_1' + W_2^NZ_2' + \ldots + W_M^NZ_M' \tag{8}$

here, Z_i', $i = 1, 2, \ldots, M$, is the ith normalized objective function value and M is the number of objectives. A_i^j, $i = 1, 2, \ldots, M$ and $j = 1, 2, .., N$, is the fuzzy set corresponding to the ith normalized objective, which is represented by a fuzzy membership function (MF) in the jth fuzzy rule; and N is the total number of the fuzzy rules. W_i^j is the weight corresponding to the ith objective in the jth fuzzy rule and $Z^j = \sum_{i=1}^M W_i^jZ_i'$ is the consequence of the jth rule.

In the pre-optimization process, a parallel single-objective optimization is implemented over all objective functions. Hence, the bounds of the objectives can be found in this process. Additionally, in this process, a set of objective values is generated for each of the

objectives, each of which is divided into three sets labeled by high, middle, and low classes. Then, the statistical parameters of these sets are all extracted to facilitate the algorithm to find out the fuzzy membership function parameters involved in the SFIS rules. For more information about the way to make the membership function parameters dependent on the statistical parameters of the objectives, we refer the readers to Rezaei et al. (2017a). Furthermore, a product-based Larsen implication function is employed to aggregate the fuzzy membership function values calculated for each premise of a certain rule to impose a weight on the consequence of that rule. Finally, the weighted average based defuzzification method is chosen for aggregating the consequences of all the fuzzy rules as follows:

$$DI = \frac{\sum_{j=1}^{N} \mu^j Z^j}{\sum_{j=1}^{N} \mu^j} \qquad (9)$$

where μ^j is the aggregated membership degree that is assigned to consequence Z^j for the jth fuzzy rule of the SFIS, which is calculated by the following equation: $\mu^j = f_1^j \times f_2^j \times \ldots \times f_M^j$. Here, f_i^j is the membership degree that is assigned to the ith normalized objective function value in the jth rule, and $Z^j = W_1^j Z_1' + W_2^j Z_2' + \ldots + W_M^j Z_M'$, where $i = 1, 2, \ldots, M$. DI is called the comprehensive Dominance Index. Table 2 illustrates a scheme for defining the weight vectors for a bi-objective problem and depicts an

Table 2 MFs combinations in the rules of the SFIS for a bi-objective problem assuming the weight step = 0.1

W_1	W_2	Z_1'/Z_2'			
0	1	High/mid	High/low	Mid/low	Low/low
0.1	0.9	High/mid	High/low	Mid/low	Low/low
0.2	0.8	High/mid	High/low	Mid/low	Low/low
0.3	0.7	High/mid	High/low	Mid/low	Low/low
0.4	0.6	High/mid	High/low	Mid/low	Low/low
0.5	0.5	–	–	–	Low/low
0.6	0.4	Low/mid	Low/high	Mid/high	Low/low
0.7	0.3	Low/mid	Low/high	Mid/high	Low/low
0.8	0.2	Low/mid	Low/high	Mid/high	Low/low
0.9	0.1	Low/mid	Low/high	Mid/high	Low/low
1	0	Low/mid	Low/high	Mid/high	Low/low

effective way to combine the fuzzy membership functions regarding the weight vectors. In a bi-objective minimization problem, the DI in Eq. (9) mostly tends to the Z^j calculated as $Z^j = W_1^j Z_1' + W_2^j Z_2'$, in which a specific relation expressed as $\frac{W_1^j}{W_2^j} \cong -\frac{\partial Z_2'}{\partial Z_1'}$, is held between (W_1^j, W_2^j) and (Z_1', Z_2'). The more extreme a solution with the location of (Z_1', Z_2') in the objective space, the less the most tended Z^j value, where $j = 1, 2, \ldots, NR$, and NR stands for the number of the SFIS rules. Meanwhile, the less the most tended Z^j value, the less the value of DI will be. Therefore, the more extreme solutions in the objective space are always assigned the less DI values. Since the extreme solutions, which indeed, are the endpoints on a non-dominated front, could frequently guide the other solutions to the solutions having the less objective values and produce the better non-dominated fronts, these solutions must be chosen as the guide solutions when decided to select the $Pbest$ or $Gbest$ solutions in this algorithm.

Furthermore, the DI not only determines the best solution (the most extreme one) among several non-dominated solutions on a local Pareto front but is capable of preferring the dominated and non-dominated solutions in the comparisons performed to delineate the guide solutions. In fact, in a minimization problem, every weighted average of the lower values of Z^j presented by a non-dominated solution is lower than that of the higher values of Z^j presented by a dominated one. As a result, the lower the DI of a solution, the better that solution in terms of both extremity and dominance.

In every iteration of f-MOPSO, the particle having the lowest DI between the current $Pbest$ particle and the newly updated ones determines the new $Pbest$, and the lowest DI obtained from all $Pbests$ of the swarm delineates the $Gbest$ particle in that iteration. The other calculations are the same as in a single-objective PSO. Moreover, the non-dominated solutions obtained from each iteration are stored in an external archive as the final solutions found by the algorithm, forming the final Pareto front.

Proposed diversity-enhanced fuzzy multi-objective PSO

The f-MOPSO/Div is an improved version of the f-MOPSO algorithm designed upon some improvements made to the original f-MOPSO. These advancements

can be briefly mentioned as follows: (1) the diversity-based *Gbest* selection, (2) the mutation-aided global search strengthening that is only recommended for solving the large-scale optimization problems, and (3) removing the pre-optimization process. These advancements are listed below and explained in detail.

Diversity-based Gbest selection

The PSO and f-MOPSO algorithms all face the premature convergence problem in their original versions. This problem emerges when the search for the higher-fitness areas in the search space would be at the cost of losing extremity among the particles in the swarm of particles. To tackle this problem, in f-MOPSO/Div, the non-dominated *Pbest* particles are all extracted from the swarm, and the one that is located in the least-densely populated region is chosen as the *Gbest*. The diversity of a particle can be calculated as follows.

$$d_i = \min_j \sum_{k=1}^{M} \left| f_k^i(x) - f_k^j(x) \right| \qquad (10)$$

where $i = 1, 2, \ldots, N_{nd}; j \in \{1, \ldots, i-1, i+1, \ldots, N_{nd}\}$; M = number of objectives; $f_k^i(x)$ = kth objective for the ith solution and $f_k^j(x)$ = kth objective for the jth solution. Also, d_i is the diversity index of the ith particle. Note that when calculating this index, $i \neq j$. N_{nd} is the number of non-dominated *Pbest* particles. The *Gbest* would be the non-dominated *Pbest* having the highest diversity index. This approach to choosing the *Gbest* particle can effectively prevent one end of the Pareto front from being more focused and can ensure a nice balance and make the solutions fluctuate among all ends of the local Pareto fronts to entirely identify the objective space.

Mutation-aided local optima avoidance

To enhance the performance of the f-MOPSO and avoid the particles to be trapped in local optima, we propose using a mutation mechanism. Among a number of the mutation mechanisms, an adaptive polynomial mutation is addressed here. The polynomial mutation (Deb and Deb 2014) is a kind of mutation that transfers a particle from one location to another location by assuming that the probability of the particle's transfer to closer locations is higher than that of the particle's transfer to farther locations in the search space. Furthermore, in f-MOPSO/Div, the mutation probability is assumed to be a dynamic probability

rather than a fixed one in the optimization process. In such a mechanism, the mutation probability is high in the early iterations, and linearly decreases by lapse of iterations. The dynamic mutation probability can be calculated as follows:

$$p_m = p_{m,\max} - \frac{p_{m,\max} - p_{m,\min}}{iter_{\max}} \times iter \qquad (11)$$

where $p_{m,\max}$ and $p_{m,\min}$ are the maximum and minimum values of the mutation probability that is set at the beginning of optimization, respectively; $iter$ is the number of the current iteration; $iter_{\max}$ is the maximum number of iterations; and p_m is the probability of mutation. The polynomial mutation implementation is allowed once the random number generated for each decision variable (r_m) is lower than the dynamic mutation probability (p_m) at each iteration. Therefore, the mutation value is calculated as follows:

$$\delta_i = \begin{cases} (2r_i)^{1/(\eta_m+1)} - 1 & ; if\ r_i < 0.5 \\ 1 - \left[(2(1-r_i))^{1/(\eta_m+1)} \right] & ; if\ r_i \geq 0.5 \end{cases} \qquad (12)$$

where r_i is a random number that is generated for the ith decision variable of a focused particle upon which ($r_m < p_m$); η_m is the distribution index of mutation, which is usually set to a constant number; and δ_i is the mutation value. Then, the ith decision variable is mutated as follows:

$$x_{i,\text{new}}^t = x_{i,\text{old}}^t + \delta_i (Ub_i - Lb_i) \qquad (13)$$

where $x_{i,\text{new}}^t$ is the mutated value of the ith decision variable, $x_{i,\text{old}}^t$ is the previous value of the ith decision variable, and Ub_i and Lb_i are the upper bound and lower bound of the ith decision variable, respectively.

Removing pre-optimization process

The important and preliminary process in the f-MOPSO is the pre-optimization process. However, the pre-optimization can be very time-consuming and imprecise, especially when handling large-scale multi-objective optimization problems. Furthermore, this process could negatively impact the quality of the optimization results by imparting more importance to an objective that is much closer to its ideal/minimum value than other objectives. In f-MOPSO/Div, this process is removed from the algorithm and incorporated into the main

structure of the f-MOPSO/Div. In this way, the necessary parameters are calculated and extracted iteration by iteration. In this way, not only the optimization process is going well but also the computational costs can also be considerably mitigated.

The flowchart of the f-MOPSO/Div algorithm is shown in Fig. 1.

Experimental results on standard benchmark functions

Comparative algorithms and parameter setting

To validate the proposed f-MOPSO/Div, here, this algorithm is compared with the original f-MOPSO and two popular multi-objective evolutionary optimization algorithms i.e. non-dominated sorting

genetic algorithm-type II (NSGA-II), first proposed by Deb et al. (2002), as the most popular multi-objective genetic algorithm (MOGA) and the speed-constrained multi-objective particle swarm optimization (SMPSO) algorithm, first introduced by Durillo et al. (2009), as a robust multi-objective PSO algorithm (MOPSO).

All algorithms are applied to seven lower-dimensional benchmark problems and seven higher-dimensional and more complex benchmark problems proposed in the Congress on Evolutionary Computation (CEC2009) (Zhou et al. 2009). All of the objectives in these problem suites are to be minimized, except for the Kita problem, in which the objectives are to be maximized. These problems cover a variety of challenges for multi-objective optimization algorithms, having continuous, discontinuous, linear, and non-linear, concave, and convex optimal Pareto fronts. Furthermore, three
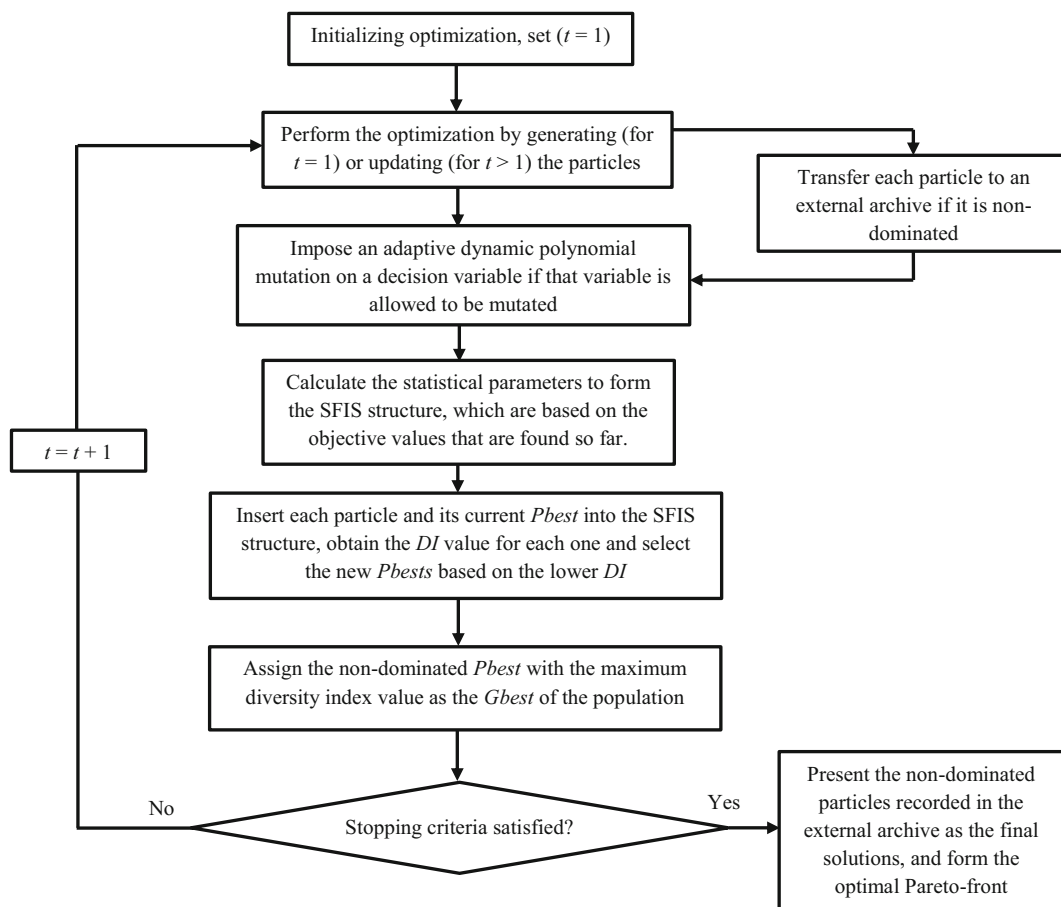

Fig. 1 Flowchart of f-MOPSO/Div

out of seven low-dimensional problems are constrained and others are non-constrained.

For comparison of the algorithms introduced in this section, the tunable parameters of these algorithms should be the first set. For NSGA-II, the crossover probability is set to 0.9, and the mutation probability is set to 0.1 for low-dimensional problems and $1/D$ for high-dimensional problems, in which D is the number of decision variables of each problem. Furthermore, η_c and η_m are both set to 20. The size of the tournament selection is also set to 2, and the size of the pool of the elite chromosomes is set to half of the population size. For SMPSO, the size of the archive is set to be the same as the population size and η_m is set to 20. For f-MOPSO and f-MOPSO/Div, the weight step is set to 0.1 to form the weight combinations and η_m is set to 20. Furthermore, $k_{\max}$ and $k_{\min}$ are set to 0.9 and 0.4, respectively. In f-MOPSO/Div, for UF1, UF4, UF5, UF6, and UF7 test problems, $p_{m,\ \max}$ and $p_{m,\ \min}$ are set to 0.1 and 0.01, respectively, and for UF2 and UF3 these parameters are set to 0.01 and 0.001, respectively. For doing a fair comparison, all algorithms are going on until maximum 200 iterations. Furthermore, the population size of all algorithms is set to 40.

Performance metric

To determine the best-performing multi-objective algorithm, the performance of each algorithm should be evaluated under a comprehensive criterion. Here, the performance of all competitive algorithms over all benchmark problems is compared based on the inverted generational distance (IGD), first proposed by Sierra and Coello (2005). The IGD metric can be able of evaluating the eligibility of the optimization algorithms in terms of both convergence and diversity of the final solutions the algorithms found (Zhou et al. 2009) and is calculated as follows:

$$IGD = \frac{1}{N}\sqrt{\sum_{i=1}^{N}d_i^{\ 2}} \tag{14}$$

where d_i is the Euclidean distance between the ith member of the known optimal Pareto front and the nearest member of the final Pareto front found by the algorithms, and N is the size of the optimal Pareto set for each problem.

Comparison of the algorithms on benchmark test problems

In this section, the capabilities of the proposed f-MOPSO/Div algorithm are evaluated against those of NSGA-II, SMPSO, and f-MOPSO algorithms. The detailed numerical results are presented in Table 3, and four instances of the resulting Pareto fronts are illustrated in Figs. 2, 3, 4, and 5.

Note that in all of these figures, the optimal Pareto fronts achieved by NSGA-II, SMPSO, f-MOPSO, and f-MOPSO/Div are presented in the subfigures (a), (b), (c), and (d), respectively. As can be seen in Table 3, the f-MOPSO/Div significantly outperforms its competitors in 22 out of 28 (79%) cases considered as the performance criteria (average, best, worst, and std (standard deviation) of IGD metric obtained over numerous independent runs).

For much more challenging the capabilities of the proposed algorithm, all algorithms were implemented on 30-dimensional complex UF benchmark problems. The detailed numerical results are presented in Table 4. In general, the proposed f-MOPSO/Div is successful in achieving better results on 19 out of 28 (68%) of the performance criteria, compared to other competitors, while each of NSGA-II and SMPSO algorithms can reach better results only on 4 out of 28 (14%) of the criteria.

Conjunctive surface-ground water use management

Study area

The Gavkhouni river basin covering an area of 41,547 km^2 is located at the Central Plateau river basin in Iran. The basin is including 21 sub-basins. The study area is Najafabad Plain located in west-central Iran as a part of Zayandeh-Rud River Basin located in the greater Gavkhouni river basin. This plain is 1712 km^2 area, with geographical coordinates between 50° 33′ 32″ to 51° 40′ 00″ Eastern longitudes and 32° 19′ 14″ to 33° 00′ 32″ Northern latitudes (Fig. 6). Read more about this basin in (Safavi and Rezaei 2015).

The Najafabad aquifer occupies an area of 940.9 km^2 including 14,623 wells with an annual discharge of 852.7 million cubic meters (MCM) (Yekom Consulting Engineers 2013). This aquifer

Table 3 Statistical results for *IGD* metric on the low-dimensional standard benchmark functions. (The results corresponding to the best-performing algorithms are italicized)

Problem	Performance criteria	NSGA-II	SMPSO	f-MOPSO	f-MOPSO/Div
Constr-Ex	Average	1.8930E−01	1.0670E−01	1.4992E−01	*6.1049E−02*
	Best	1.2595E−01	5.1443E−02	8.9892E−02	*2.6053E−02*
	Worst	3.7416E−01	1.9271E−01	2.2699E−01	*1.4204E−01*
	Std	7.5622E−02	4.4863E−02	*3.4661E−02*	4.2011E−02
Fonseca	Average	2.0818E−01	2.2257E−01	2.6438E−01	*4.0065E−02*
	Best	1.0073E−01	1.3941E−01	1.6261E−01	*1.5292E−02*
	Worst	2.7110E−01	3.4401E−01	3.3685E−01	*1.0706E−01*
	Std	5.0004E−02	6.3290E−02	5.3556E−02	*2.9516E−02*
Kita	Average	1.2790E+00	3.2972E−01	3.1450E−01	*7.1611E−02*
	Best	4.1840E−01	2.7230E−01	1.5763E−01	*4.5432E−02*
	Worst	3.1099E+00	3.9296E−01	5.4031E−01	*1.3337E−01*
	Std	7.7696E−01	4.0356E−02	1.2065E−01	*2.4527E−02*
Binh	Average	9.6489E−01	3.9032E−01	8.9423E−01	*3.4556E−01*
	Best	6.8518E−01	2.4507E−01	7.3413E−01	*5.8164E−02*
	Worst	1.2895E+00	*7.6926E−01*	1.2968E+00	1.1366E+00
	Std	2.0802E−01	*1.6724E−01*	1.7944E−01	3.4069E−01
DTLZ2	Average	2.5770E−01	2.7602E−02	8.4346E−02	*4.4857E−03*
	Best	1.8291E−01	1.5672E−02	5.5225E−02	*9.8735E−04*
	Worst	4.1627E−01	5.4613E−02	1.1455E−01	*1.5902E−02*
	Std	7.3330E−02	1.1904E−02	1.9088E−02	*4.6264E−03*
Kursawe	Average	1.7541E−01	3.1510E−01	5.2464E−01	*6.4661E−02*
	Best	1.2261E−01	1.9847E−01	1.2960E−01	*3.2606E−02*
	Worst	3.0401E−01	5.7527E−01	1.7609E+00	*1.4265E−01*
	Std	5.7320E−02	1.0865E−01	5.2333E−01	*3.3211E−02*
Deb	Average	2.3023E−01	2.7115E−01	*2.0324E−01*	2.5065E−01
	Best	1.4726E−01	1.0230E−01	9.8635E−02	*9.3955E−02*
	Worst	*2.7301E−01*	3.2112E−01	2.8947E−01	3.6764E−01
	Std	*3.5037E−02*	6.4008E−02	8.1797E−02	7.7609E−02

is mainly recharged by river water infiltration, irrigation return flow, and the direct precipitation on the plain; however, the annual precipitation in this area is very low, and the main surface water recharging the Najafabad aquifer is supplied from the Zayandeh-Rud River and reservoir. The Njafabad plain is divided into two main sub-plains: (1) Nekouabad-Right located on the right bank of the Zayandeh-Rud River, and (2) Nekouabad-Left located on the Left bank of the Zayendeh-Rud River.

Due to the consumption of the largest volume of available water resources and the massive agricultural and horticultural productions, the Najafabad sub-basin, including Nekouabad-Right and Nekouabad-Left sub-areas, is identified as the most important sub-basin of the Gavkhouni basin, such that 584 thousand tons of agricultural products and 45.8 thousand tons of horticultural products are annually yielded in this sub-basin. The agricultural sector is the most water-consuming in the region, and any water resources management plan in the Najafabad region should properly address the agricultural water use in this region.

The Najafabad region is mainly an irrigated agricultural area, mainly due to lacking adequate
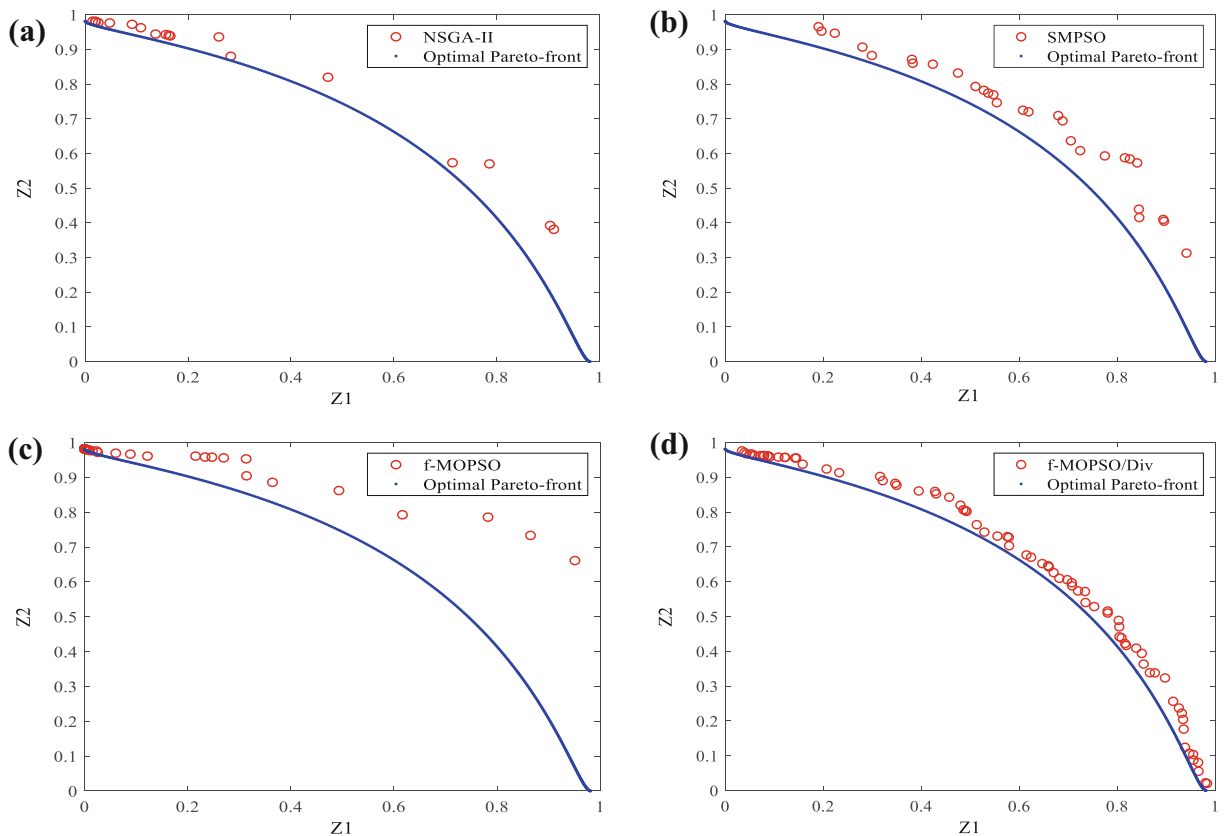
Fig. 2 Pareto fronts resulting from **(a)** NSGA-II; **(b)** SMPSO; **(c)** f-MOPSO; and **(d)** f-MOPSO/Div algorithms applied to Fonseca problem

precipitation in the region, making this region be categorized in the semi-arid regions. The predominant crops cultivated in this area consist of wheat and barley, with 41.8% of the total area, and rice and alfalfa with 14.5% and 5.5% of total cultivated area, respectively. Potato and onion are also desired crops cultivated in this area, mainly in the autumn season (Yekom Consulting Engineers 2013; Zayandab Consulting Engineers 2008).

Decreased reliable surface water resources in the region as a result of a streak of droughts which have occurred in recent years poses challenges in surface water supply for this region, imposing much more pressure on groundwater resources to meet increasing agricultural demands in this region, such that the groundwater level in the Nekouabad-Right and Nekouabad-Left regions experiences the drastic 13 and 20 m drawdown in just a decade. Moreover, the increasing population as well as some negative climate change impacts

such as global warming prompt the water demands to be increased in this region. This increasing negative balance between water supply and water demands in such a semi-arid region urges water resources management for this region. Furthermore, while an averagely 7.4% of total water consumption in the agricultural sectors in the country is used in this region, this region yields just a ratio of 4.6% of total national agricultural net benefits.

Accordingly, in this paper, we aim at developing a management model for optimizing conjunctive surface-ground water use. This optimal management model is developed with two main goals: (1) minimizing the groundwater withdrawals and (2) maximizing the crop yields as a solution to enhancing the net benefits of the agricultural activities in the study area. In this study, a 13-year planning period beginning from 2003–2004 water year through 2015–2016 water year is considered as the planning period.
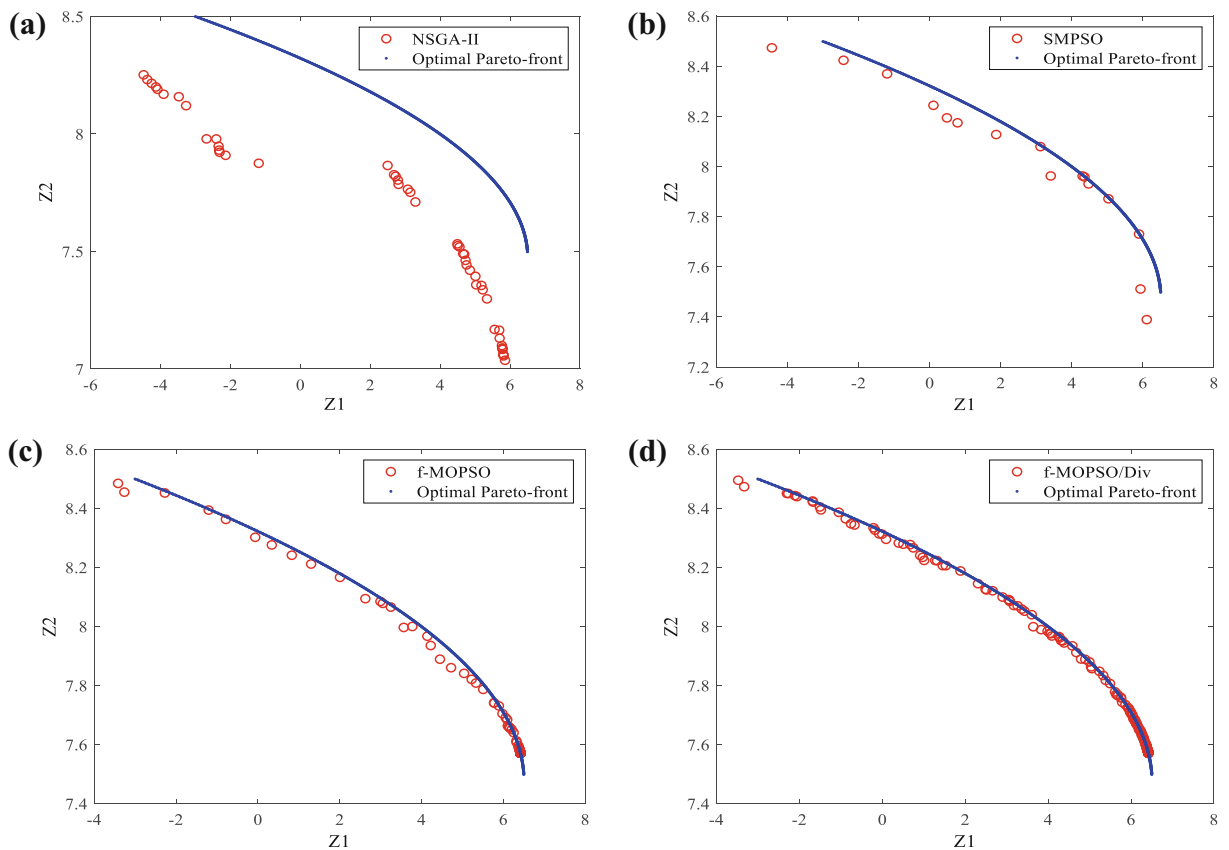
Fig. 3 Pareto fronts resulting from **(a)** NSGA-II; **(b)** SMPSO; **(c)** f-MOPSO; and **(d)** f-MOPSO/Div algorithms applied to Kita problem

Optimization model mathematical formulation

$$
\text{Minimize } Z_1 = \sum_{i=1}^{13} \left[\frac{\left(\sum_{j=1}^{12} \Delta H_{ij} - \Delta H_{i,\text{opt}}\right)^2 / 2 -}{\left(\sum_{j=1}^{12} \Delta H_{ij} - \Delta H_{i,\text{opt}}\right)^2 / 2 \times sgn\left(\sum_{j=1}^{12} \Delta H_{ij} - \Delta H_{i,\text{opt}}\right)} \right] + Z_{\text{pen1}} + Z_{pen2} \tag{15}
$$

$$
sgn\left(\sum_{j=1}^{12} \Delta H_{ij} - \Delta H_{i,\text{opt}}\right) = \left| \sum_{j=1}^{12} \Delta H_{ij} - \Delta H_{i,\text{opt}} \right| / \left(\sum_{j=1}^{12} \Delta H_{ij} - \Delta H_{i,\text{opt}}\right) \tag{16}
$$

$$
Z_{\text{pen1}} = m_1 \times \left| \min_i \left\{ \min\left[sgn\left(GW_{\text{total,max}} - \sum_{j=1}^{12} GW_{ij}\right), 0 \right] \right\} \right| ; for\ i = 1, 2, \ldots, 13. \tag{17}
$$

$$
Z_{\text{pen2}} = m_2 \times \left| \min\left[sgn\left(\sum_{i=1}^{13}\sum_{j=1}^{12} \Delta H_{ij} - \Delta H_{\text{total,min}}\right), sgn\left(\Delta H_{\text{total,max}} - \sum_{i=1}^{13}\sum_{j=1}^{12} \Delta H_{ij}\right), 0 \right] \right| \tag{18}
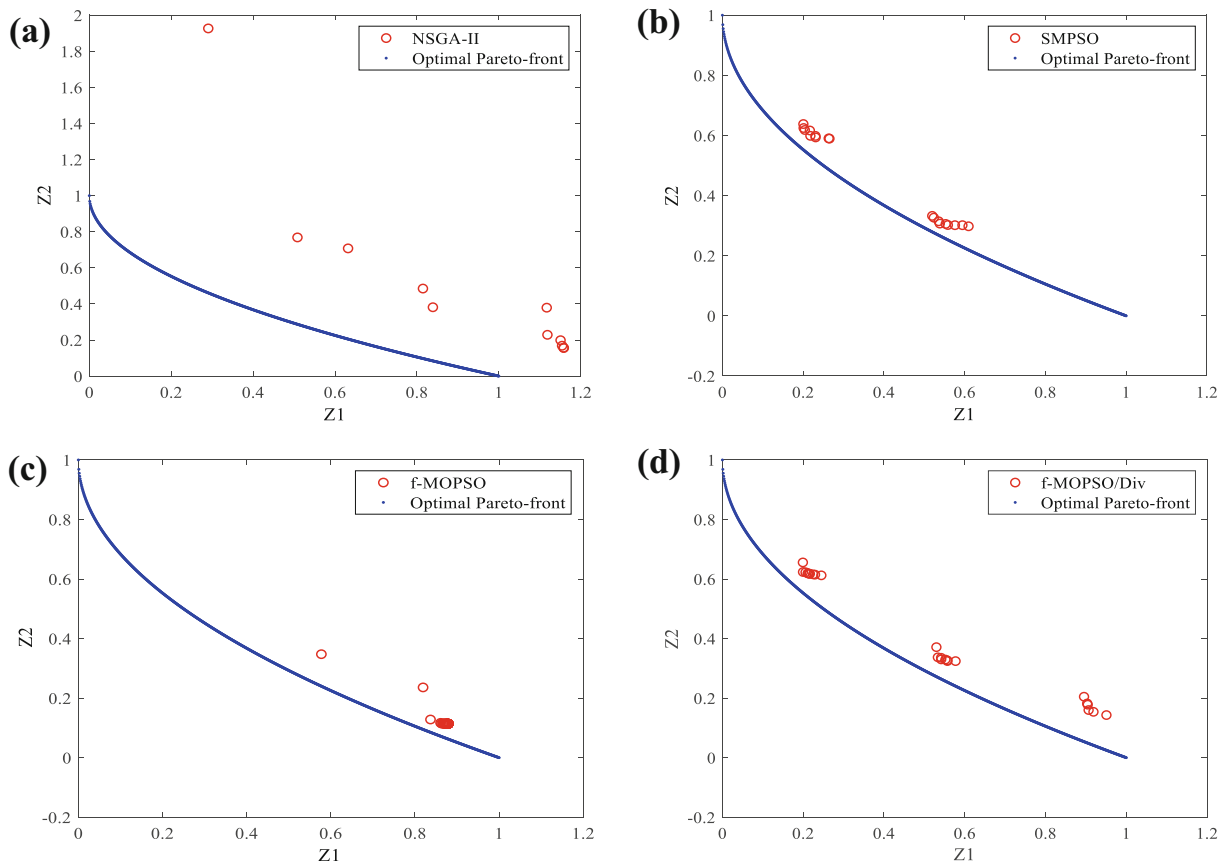$$

Fig. 4 Pareto fronts resulting from **(a)** NSGA-II; **(b)** SMPSO; **(c)** f-MOPSO; and **(d)** f-MOPSO/Div algorithms applied to UF1 problem

$$\text{Maximize } Z_2 = \sum_{i=1}^{13} \sum_{c=1}^{6} \left(Y_{ic} \times A_{ic} \right) \tag{19}$$

$$\frac{Y_{ic}}{Y_{ic,\max}} = \prod_{j=1}^{12} \left[1 - K_{y_{jc}} \left(1 - \frac{Sup_{ij}}{D_{ij}} \right) \right]; for\ i$$

$$= 1, 2, \ldots, 13 \tag{20}$$

Subject to:

$$D_{ij} = \sum_{c=1}^{6} CD_{ijc} \times A_{ic} \times 10^{-5} \tag{21}$$

$$Sup_{ij} = SW_{ij,\text{net}} + GW_{ij,\text{net}} \tag{22}$$

$$SW_{ij,\text{net}} = a \times b \times c \times SW_{ij} \tag{23}$$

$$GW_{ij,\text{net}} = a \times GW_{ij} \tag{24}$$

$$SW_{j,\min}^{\text{avail}} \leq SW_{ij} \leq SW_{j,\max}^{\text{avail}} \tag{25}$$

$$GW_{j,\min}^{\text{avail}} \leq GW_{ij} \leq GW_{j,\max}^{\text{avail}} \tag{26}$$

$$\Delta H_{\text{total,min}} \leq \sum_{i=1}^{13} \sum_{j=1}^{12} \Delta H_{ij} \leq \Delta H_{\text{total,max}} \tag{27}$$

$$H_{ij} = H_{i,j-1} - \Delta H_{i,j-1}; for\ j \neq 1 \tag{28}$$

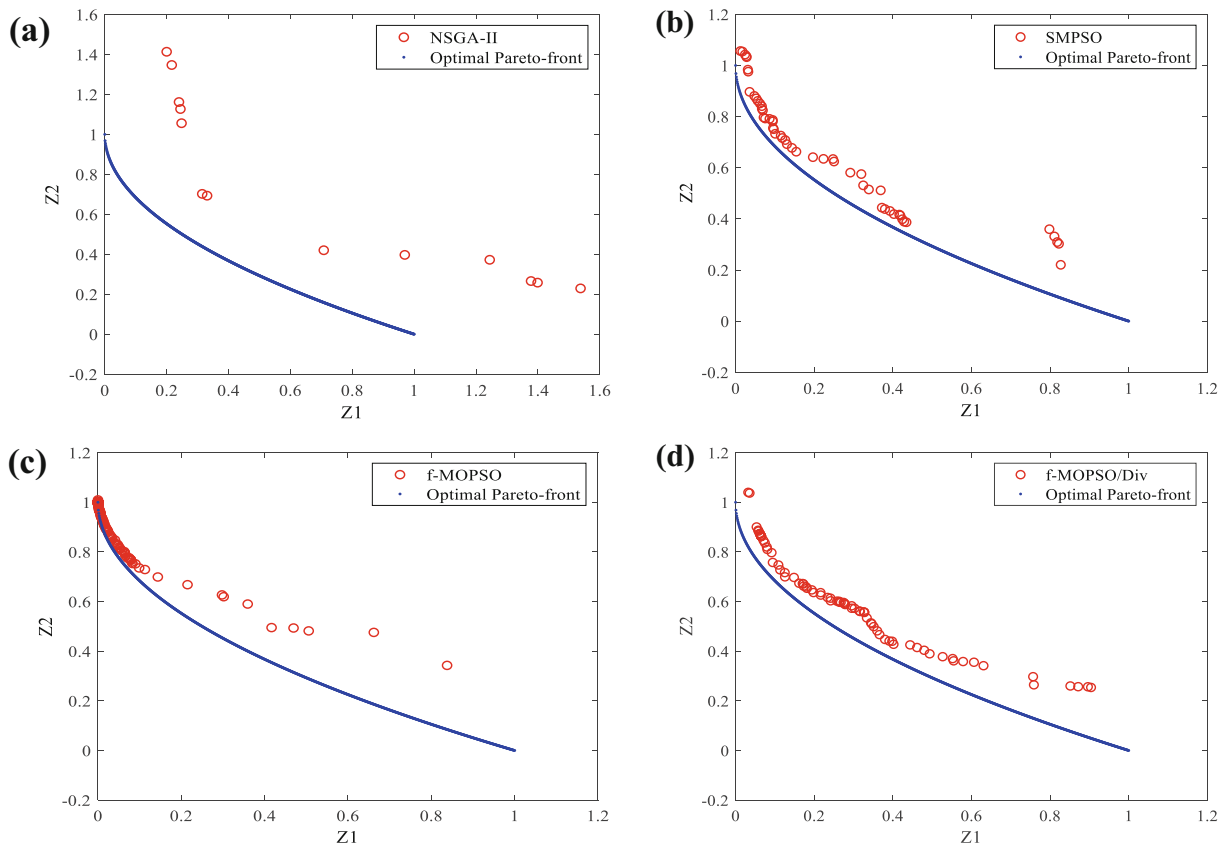$$H_{i,1} = H_{i-1,12} - \Delta H_{i-1,12} \tag{29}$$

Fig. 5 Pareto fronts resulting from **(a)** NSGA-II; **(b)** SMPSO; **(c)** f-MOPSO; and **(d)** f-MOPSO/Div algorithms applied to UF2 problem

The parameters used in the model formulation are defined in detail below:

Z_i	ith objective function ($i = 1, 2$)
Z_{pen1}	The first penalty function restricting the groundwater extraction in each study sub-area.
m_1	The penalty coefficient in the first penalty function.
D_{ij}	The net water demand of the jth month in the ith water year (MCM).
Sup_{ij}	The net water supply of the jth month in the ith water year (MCM).
A_{ic}	The cultivated area for cth crop in the ith water year (ha).
ΔH_{ij}	Groundwater level (GWL) variation in jth month of the ith water year (m).
$\Delta H_{i, opt}$	The optimal GWL variation in the ith water year (m).
Z_{pen2}	The second penalty function restricting the GWL variations over the whole planning period.

$GW_{total, max}$	The maximum allowable groundwater volume extracted in each water year (MCM).
m_2	The penalty coefficient in the second penalty function.
$\Delta H_{total, min}$	The minimum allowable GWL variation over the whole planning period (m).
$\Delta H_{total, max}$	The maximum allowable GWL variation over the whole planning period (m).
Y_{ic}	The yield per unit cultivated area of the cth crop in the ith water year (kg/ha).
H_{ij}	The initial GWL in the jth month of the ith water year (m).
CD_{ijc}	The net crop water requirement of the cth crop per unit cultivated area in the jth month of the ith water year (mm).
$GW_{ij, net}$	The net groundwater volume extracted in the jth month of the ith water year (MCM).
GW_{ij}	The gross groundwater volume extracted in the jth month of the ith water year (MCM).

Table 4 Statistical results for *IGD* metric on the high-dimensional standard benchmark functions. (The results corresponding to the best-performing algorithms are italicized)

Problem	Performance criteria	NSGA-II	SMPSO	f-MOPSO	f-MOPSO/Div
UF1	Average	3.8302E−01	2.5420E−01	4.0666E−01	*1.7766E−01*
	Best	3.2075E−01	1.5733E−01	2.0199E−01	*1.4209E−01*
	Worst	4.4442E−01	6.7222E−01	6.0365E−01	*2.1749E−01*
	Std	4.0116E−02	1.5838E−01	1.2331E−01	*2.4358E−02*
UF2	Average	3.6152E−01	1.4377E−01	2.1796E−01	*1.1819E−01*
	Best	3.2871E−01	1.0296E−01	1.7588E−01	*8.5923E−02*
	Worst	4.3388E−01	2.2515E−01	2.7207E−01	*1.5114E−01*
	Std	3.1178E−02	3.3958E−02	2.9979E−02	*1.8830E−02*
UF3	Average	4.1943E−01	4.4917E−01	4.7162E−01	*3.6706E−01*
	Best	3.5465E−01	4.2528E−01	3.0984E−01	*2.5288E−01*
	Worst	6.0195E−01	*4.8542E−01*	6.3517E−01	5.4217E−01
	Std	9.5076E−02	*1.8055E−02*	8.5575E−02	1.0707E−01
UF4	Average	*1.0411E−01*	1.9029E−01	1.9777E−01	1.1370E−01
	Best	*7.0716E−02*	1.7179E−01	1.9049E−01	1.0179E−01
	Worst	1.6231E−01	2.0445E−01	2.1511E−01	*1.5808E−01*
	Std	3.3668E−02	1.0675E−02	*7.5344E−03*	1.6533E−02
UF5	Average	2.7608E+00	1.5463E+00	3.2887E+00	*8.8455E−01*
	Best	2.4020E+00	6.8702E−01	1.9354E+00	*5.3020E−01*
	Worst	3.0644E+00	2.8757E+00	4.0740E+00	*1.3375E+00*
	Std	*1.9331E−01*	7.4479E−01	7.4177E−01	2.7266E−01
UF6	Average	1.7070E+00	6.4561E−01	7.2503E−01	*5.3050E−01*
	Best	1.4984E+00	4.8009E−01	3.7939E−01	*3.3858E−01*
	Worst	1.9130E+00	*9.5231E−01*	2.7224E+00	1.2143E+00
	Std	*1.3713E−01*	1.6800E−01	7.1035E−01	2.7004E−01
UF7	Average	4.8469E−01	4.9742E−01	8.2069E−01	*3.4566E−01*
	Best	3.4883E−01	*3.0279E−01*	5.4909E−01	3.1195E−01
	Worst	7.2139E−01	8.7917E−01	1.1746E+00	*3.6071E−01*
	Std	1.2857E−01	2.1756E−01	2.4141E−01	*1.5669E−02*

|			
$SW_{ij,\,net}$	The net surface water volume allocated to each study sub-area in the jth month of the ith water year (MCM).	$SW_{j,min}^{avail}$	The minimum volume of the surface water allocated in the jth month and derived from the historical data (MCM).
SW_{ij}	The gross surface water volume allocated to each study sub-area in the jth month of the ith water year (MCM).	$SW_{j,max}^{avail}$	The maximum volume of the surface water allocated in the jth month and derived from the historical data (MCM).
a	The efficiency coefficient of the water use in the farm, including the evaporation and infiltration to the aquifer.	$GW_{j,min}^{avail}$	The minimum volume of the groundwater extracted in the jth month and derived from the historical data (MCM).
b	The efficiency coefficient of the water transfer through the main irrigation canals.	$GW_{j,max}^{avail}$	The maximum volume of the groundwater extracted in the jth month and derived from the historical data (MCM).
c	The efficiency coefficient of the water distribution through the secondary irrigation canals.		
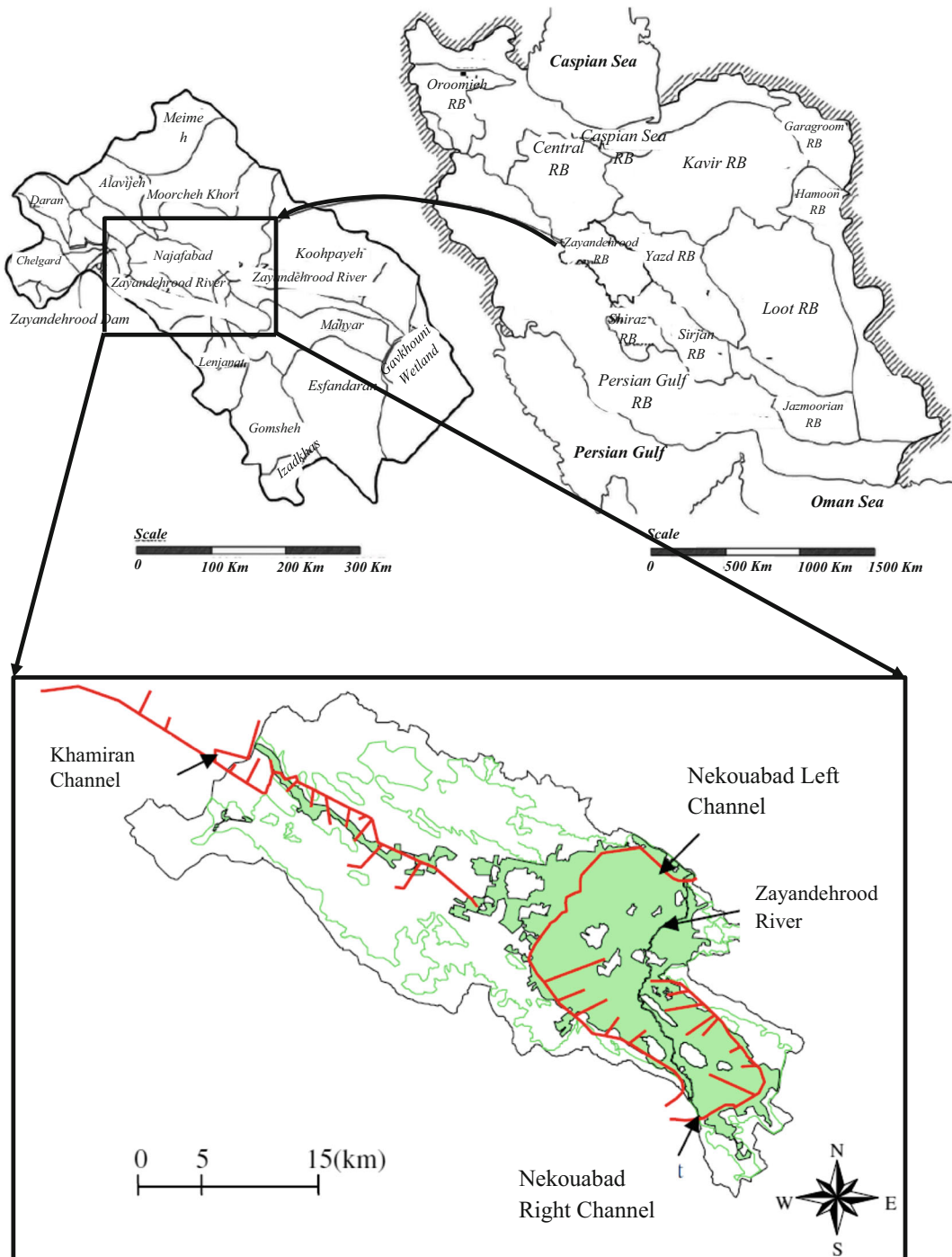
Fig. 6 Najafabad Plain in the Gavkhouni River Basin, Iran (Rezaei et al. 2017b)

$Y_{ic,\,max}$	The maximum of cth crop yield per unit cultivated area in the ith water year fulfilled when fully satisfying the crop water demand (kg/ha).	$K_{y_{ic}}$	The yield response factor of the cth crop in the ith water year, representing the crop sensitivity to the deficit irrigation.

Preparing the simulation-optimization model

Artificial neural network

A simulation-optimization model is used to solve the conjunctive use problem. In this model, the optimization section is the f-MOPSO/Div algorithm, whose superiority over other popular multi-objective evolutionary algorithms was proven in the previous sections of this paper, and the simulation model is a multi-layer perceptron feed-forward neural network (MLPFNN). The optimization model is designed to delineate the optimal surface water allocated and groundwater extracted volumes in the monthly time steps, while the simulator attempts to estimate the groundwater level (GWL) variations in any monthly time step. The MLPFNN model benefits from 286 input data series, each of which includes several input features illustrated in Figs. 7 and 8, for the Nekouabad-Right and the Nekouabad-Left regions, respectively. Fourteen input data are involved in simulating the monthly groundwater level in the Nekouabad-Right, and 13 input data are included in the Nekouabad-Left. The output of the network is the GWL variation. This variation is negative if there is GWL drawdown and is positive if the GWL rises. It is noteworthy that from the 286 data series, 65% is put aside for training the network, 10% is dedicated to validation, and 25% is assigned to the test stage. The network is adopted as a single-hidden-layer network. The 14-7-1 and 13-12-1 structures are found as the best structures for the network for the Nekouabad-Right and Nekouabad-Left sub-areas, respectively, based on numerous trials and errors. The architecture of the networks built based on the specific characteristics of each region is shown in Figs. 7 and 8.

There are several criteria to benchmark the performance of the simulators (Yeom et al. 2015; Wong et al. 2020). Among them, we adopted the correlation

Fig. 7 The architecture of the MLPFNN designed for the Nekouabad-Right region
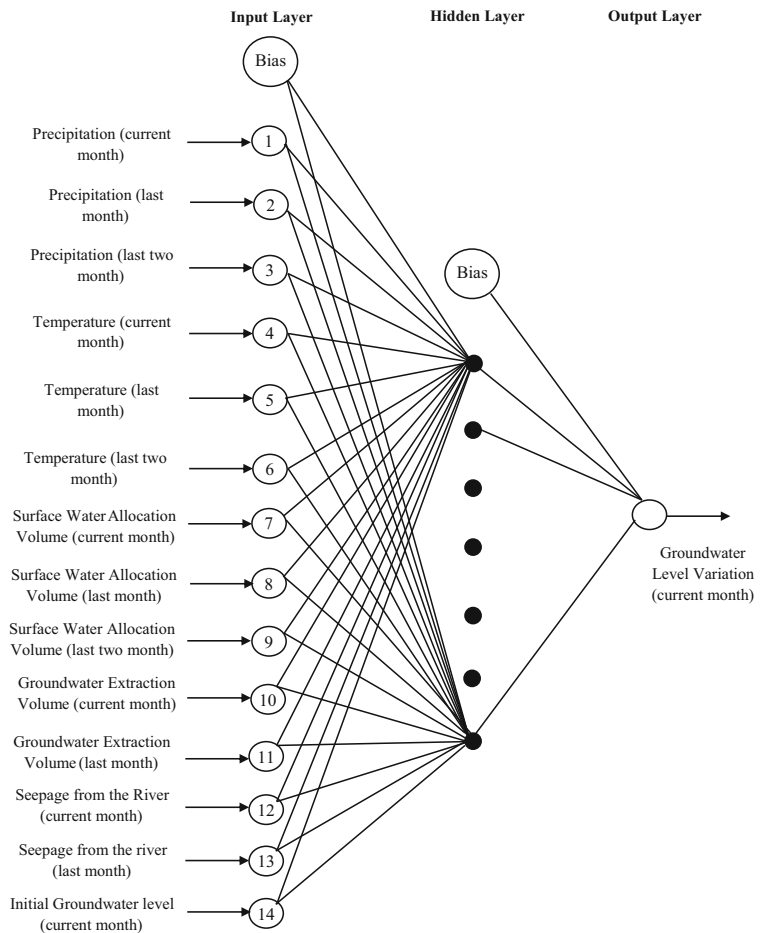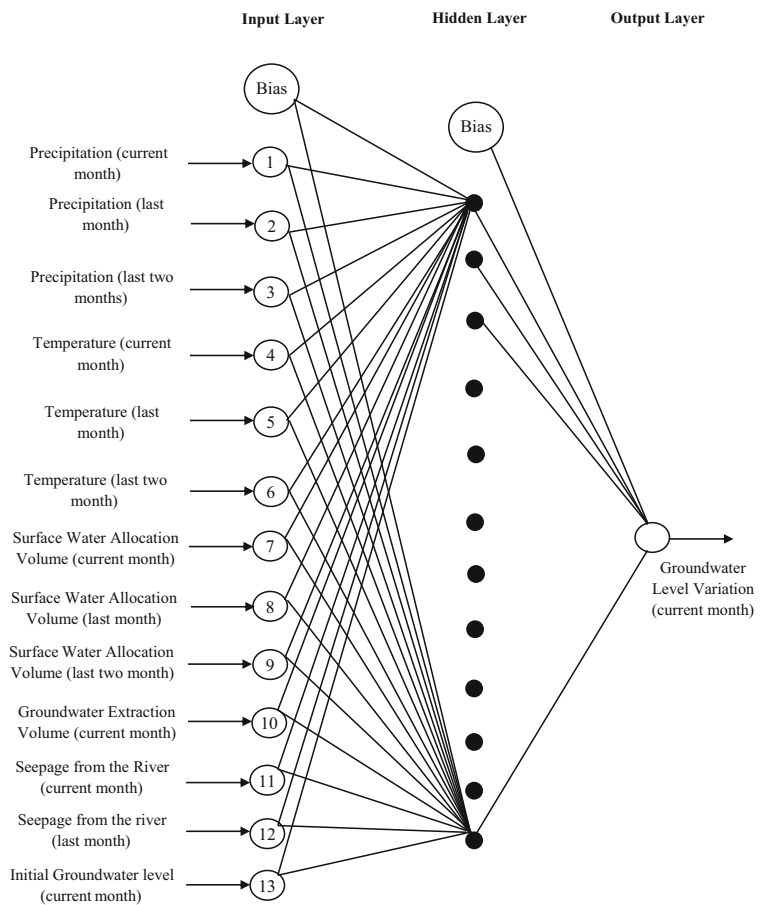
Fig. 8 The architecture of the MLPFNN designed for the Nekouabad-Left region

coefficient (R) to evaluate the goodness of fitting the simulated outputs to the observed targets. The R values resulting from the best implementation of the MLPFNN model on two study sub-areas are displayed in Table 5.

Comparison between f-MOPSO and f-MOPSO/Div

To further validate the use of the f-MOPSO/Div algorithm, the performance of this algorithm and the original f-MOPSO in solving the real-world conjunctive water use problem is investigated in this section. The maximum number of the iterations of both algorithms was set

Table 5 Correlation coefficient (R) achieved in the best implementation of the MLPFNN model

	Training	Validation	Test	Total
Nekouabad-Right	0.84	0.92	0.82	0.85
Nekouabad-Left	0.78	0.46	0.85	0.76

to 200. It is noteworthy that 50 stall iterations were also set, and the stagnation of the algorithms to generate the better ideal point for the local Pareto fronts over these stall iterations is considered as the stopping criterion for the optimization process. Furthermore, the swarm size was set to 40, and the weight step in the SFIS structure was also set to 0.1. The final Pareto fronts each algorithm yields at each study sub-area are presented in Fig. 9. It is worth mentioning that the vertical axis of these Pareto fronts is, in fact, the minus of the second objective, minimization of which means maximization of the real form of the second objective presented in the mathematical formulation of the optimization model.

Since any multi-objective optimization algorithm presents an optimal Pareto front as the final result of the optimization process, there is a need to select the best point/solution on this front as the final result of the algorithm. Here, we employ compromise programming, first introduced by Zeleny (1973), to do so. According to the compromise programming, the weighted distance of
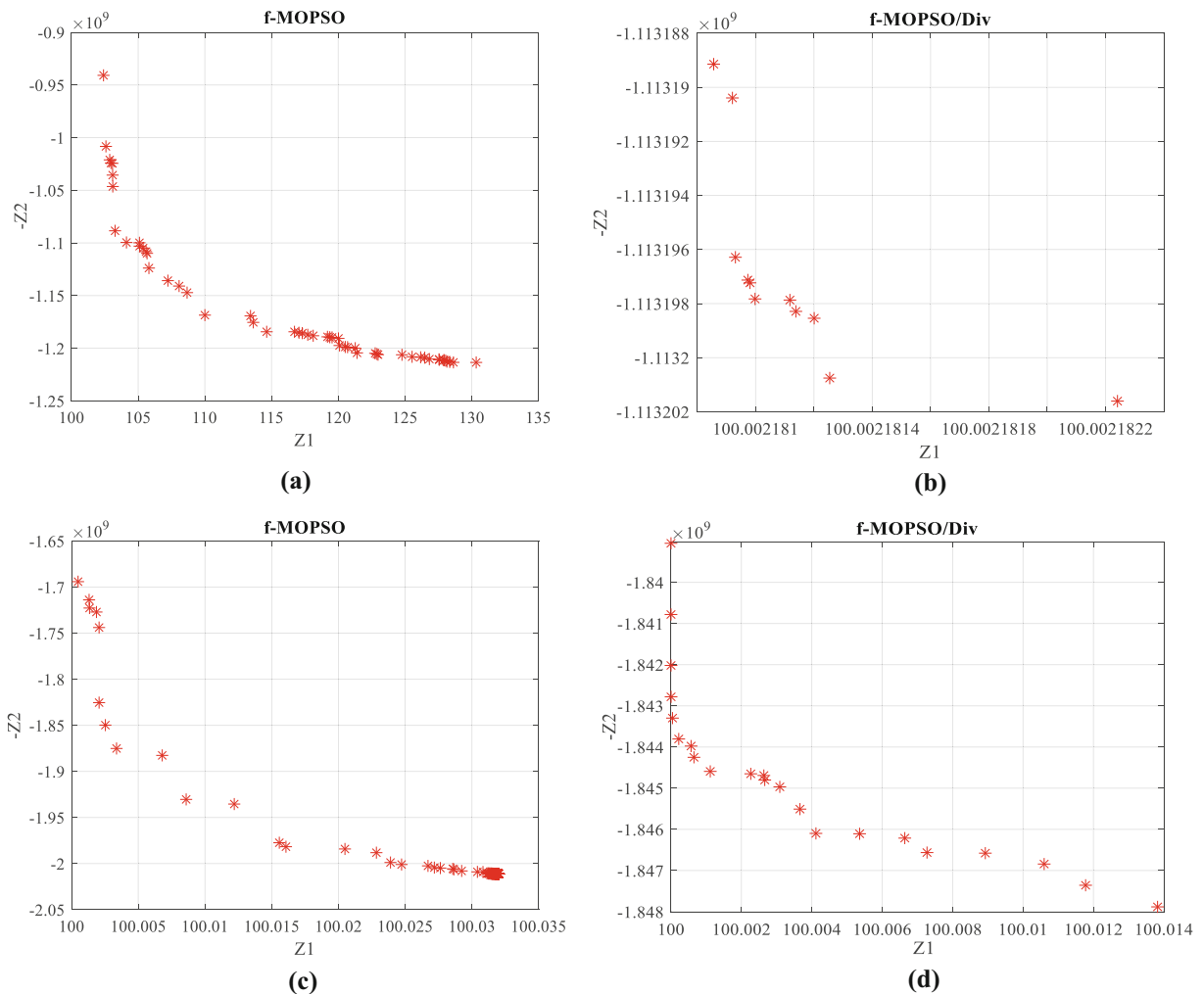
Fig. 9 Final Pareto fronts found by different algorithms in a, b right region; and c, d left region

each point to the ideal point on the Pareto optimal front can be calculated as follows:

$$D_i = \sqrt{(W_1)^2 \left(\frac{Z_1^i - Z_{1,\min}}{Z_{1,\max} - Z_{1,\min}}\right)^2 + (W_2)^2 \left(\frac{Z_2^i - Z_{2,\min}}{Z_{2,\max} - Z_{2,\min}}\right)^2} \quad (30)$$

where Z_j^i, $j = 1, 2$, is the jth objective value of the ith non-dominated solution on the final Pareto front, $Z_{j,\min}$ and $Z_{j,\max}$ are the minimum and maximum values of the jth objective on the final Pareto front, respectively, W_j is the weight assigned to the jth objective, and D_i is an index representing the weighted distance of the ith non-dominated solution on the Pareto front to the ideal solution in the objective space. To designate the weights

of the objectives, a questionnaire was filled by some of the experts and stakeholders in the field. Finally, W_1 was obtained to be 0.59 and W_2 was calculated to be 0.41.

To compare the f-MOPSO and f-MOPSO/Div algorithms in terms of their capability to solve the real-world conjunctive water use management problem, two key criteria are considered: (1) groundwater level (GWL) variations and (2) productivity. Productivity is defined as the total crop yields per unit water consumption volume (kg/m^3). The first criterion is an environmental goal, helping someone realize the performance of the algorithms to mitigate the groundwater level drawdowns to make the vital groundwater resources sustainable to exploit in the possibly dry years in the future.

Table 6 Comparison between the original and the proposed algorithms based on the performance criteria

Region	Nekouabad-Right				Nekouabad-Left			
Criterion	Drawdown (m)		Productivity (kg/m^3)		Drawdown (m)		Productivity (kg/m^3)	
Algorithm	f-MOPSO	f-MOPSO/Div	f-MOPSO	f-MOPSO/Div	f-MOPSO	f-MOPSO/Div	f-MOPSO	f-MOPSO/Div
2003–2004	− 3.18	− 1.53	0.69	0.73	3.34	2.76	1.00	1.07
2004–2005	− 2.57	− 1.52	0.88	0.85	− 1.54	− 1.44	1.03	0.96
2005–2006	− 1.30	− 1.52	0.89	0.84	2.83	2.88	0.95	0.91
2006–2007	1.87	− 1.49	0.91	0.86	− 1.57	− 1.49	0.95	1.01
2007–2008	− 2.37	− 1.51	0.65	0.65	− 1.32	− 0.92	0.71	0.60
2008–2009	− 1.72	− 1.51	0.61	0.61	− 1.50	− 1.53	0.81	0.90
2009–2010	− 0.72	− 1.26	0.54	0.80	0.00	− 0.96	0.56	0.95
2010–2011	− 2.05	− 1.51	0.76	0.74	− 0.10	− 0.76	0.73	0.48
2011–2012	− 0.98	0.06	0.81	0.67	− 0.92	0.25	0.51	0.59
2012–2013	− 1.85	− 0.90	0.72	0.74	1.08	3.82	0.81	0.89
2013–2014	3.44	4.13	1.39	1.41	1.92	1.32	1.73	1.49
2014–2015	3.69	1.33	0.92	1.02	− 1.09	− 1.50	1.28	1.19
2015–2016	− 2.28	− 1.29	0.60	0.65	− 1.53	− 0.95	0.83	0.87

The second criterion is a comprehensive socio-economic-environmental goal, suggesting that the economic benefits achieved are at the cost of using how much water, especially the groundwater.

Tables 6 and 7 summarize the numerical values of these performance criteria achieved by the best solution obtained through the optimization. As can be seen, the f-MOPSO/Div can achieve lower GWL drawdowns over the 13-year planning period while maintaining productivity in a more desirable level as compared to the f-MOPSO algorithm. In detail, the proposed algorithm has calculated the GWL drawdown in the Nekouabad-Right region by 15% less than that computed by the f-MOPSO, while the GWL drawdown is turned into GWL rise in the Nekouabad-Left as computed by the f-MOPSO/Div, experiencing the sustainable conditions nearly 5 times more than those reported by the original f-MOPSO as the results in Table 7 illustrate.

Additionally, the results suggest slightly better productivity calculated by the proposal than that resulting from the original f-MOPSO. Since the f-MOPSO/Div shows better results to solve such a real-world environmental problem, we show some more results received from running this algorithm in the forms of figures and tables and make some discussions on these results to further enhance the understanding of the performance of this new algorithm when facing such a problem in the next section.

Results and discussion (f-MOPSO/Div application)

Nekouabad-Right

The results of the simulation-optimization model applied to the Nekouabad-Right study sub-area suggest that this region mostly relies on the groundwater

Table 7 Overall comparisons between the original and the proposed algorithms based on the major criteria

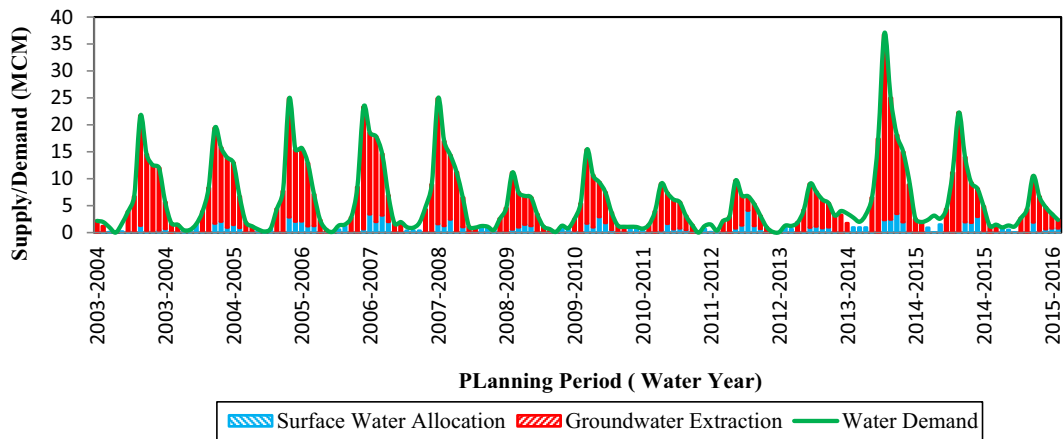| Criterion	Cumulative drawdown (m)		Average productivity (kg/m^3)	
Algorithm	f-MOPSO	f-MOPSO/Div	f-MOPSO	f-MOPSO/Div
Nekouabad-Right	− 10.02	− 8.51	0.80	0.81
Nekouabad-Left	− 0.39	1.46	0.91	0.92

Fig. 10 Surface water and groundwater allocated to the Nekouabad-Right region and the water demands

resources to supply the water demands, such that the average ratio of the groundwater extraction to the surface water allocation (GW/SW) reaches 5.75, over the whole planning period, while this figure is observed to be 12.7 in the actual operation. In the first 4 years of the planning period, the GW/SW is high, which is accompanied by the proper precipitation and the high rate of recharge by the river, and thus, the GWL drawdown could be suitably controlled over these years. Moreover, nearly 94% of the total water demands are met in these years, resulting in the productivity (total crop yields/total water consumption) equal to 0.82 kg/m^3 as a figure very similar to the average productivity observed in the actual operation in the basin. It is noteworthy that the monthly crops water demands are all calculated using the CROPWAT 8.0 software.

In conclusion, in the Nekouabad-Right study sub-area, 91% of the demand is averagely met, and the cumulative − 8.51-m GWL drawdown is achieved versus − 13.37-m drawdown seen in the actual operation of the region in the same period. Furthermore, the water productivity is calculated to be 0.814 kg/m^3 compared to 0.841 kg/m^3 averagely seen in the actual operation in the basin, suggesting the desired balance between the economic aspect of the conjunctive use, reflected by the crop yields, and the environmental aspect, reflected by the water consumption. Also, the ratio of the groundwater extraction to the surface water allocation is set to be 5.75, whereas this figure is seen to be 12.7 in the actual operation, suggesting a 55% decrease in this ratio, which in turn can hold a suitable balance between the recharging and discharging factors of the aquifer
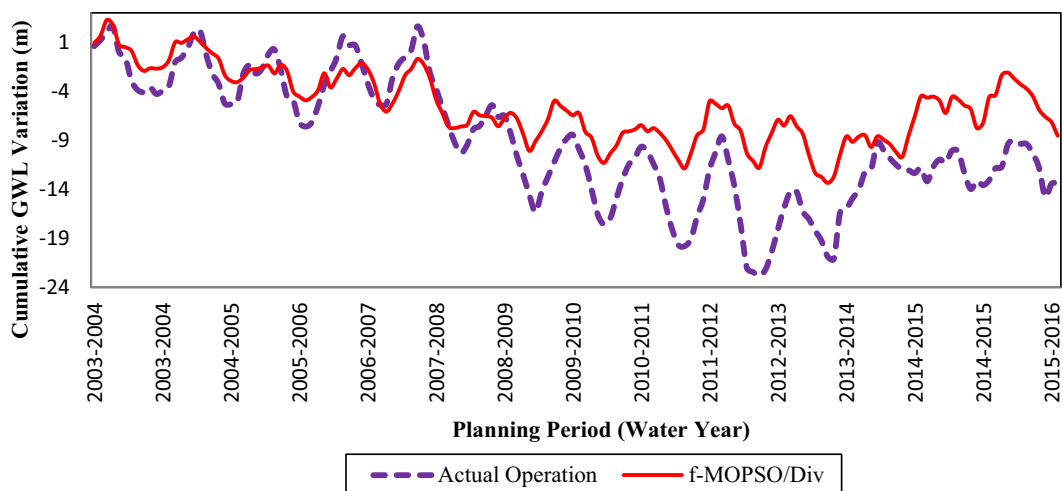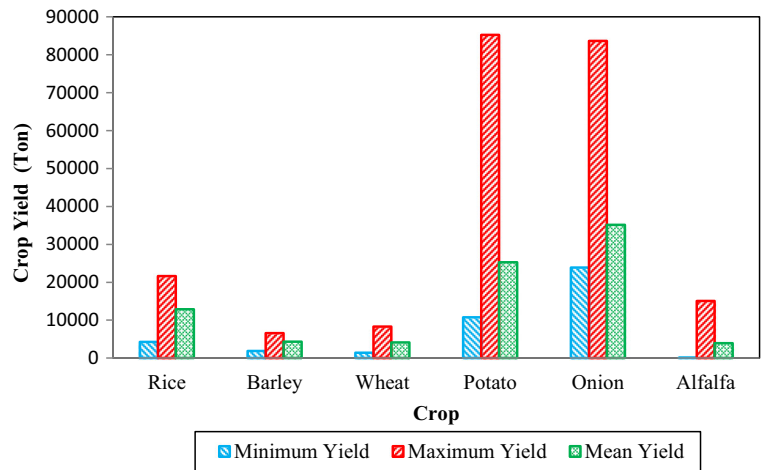

Fig. 11 Cumulative groundwater level variation in the Nekouabad-Right region

Fig. 12 Crop yield for the dominant crops over the whole planning period for the Nekouabad-Right region

resulting in a desirable GWL drawdown over the whole 13-year planning period. It is noteworthy that since only six dominant crops among a large variety of the crops are considered to be cultivated in the study area in this paper, we reduced the groundwater and surface water volumes available to the crops, based upon the amount of the reduction of the total water demands to the demands determined for the dominant crops. This procedure can make all comparisons based on the water ratio met, GWL variations, and the ratio of the groundwater to surface water allocation absolutely fair and plausible in this paper. This revision on the water resources available is also made in the Nekouabad-Left region.

Figure 10 shows the volume of the water supply separated by surface-ground water along with the demands. Figure 11 depicts the cumulative GWL drawdown delineated by the proposed model versus what is seen in the actual operation. Figure 12 displays a statistical chart presenting the six main crop yields over the whole planning period, and finally, Fig. 13 illustrates the ratio of the groundwater extraction to the surface water allocation separated by different water years compared to the actual operation, all in the Nekouabad-Right region.

Nekouabad-Left

The results obtained in this region suggest the average groundwater extraction to the surface water allocation to be 3.98 versus a value of 8.00 observed in the actual
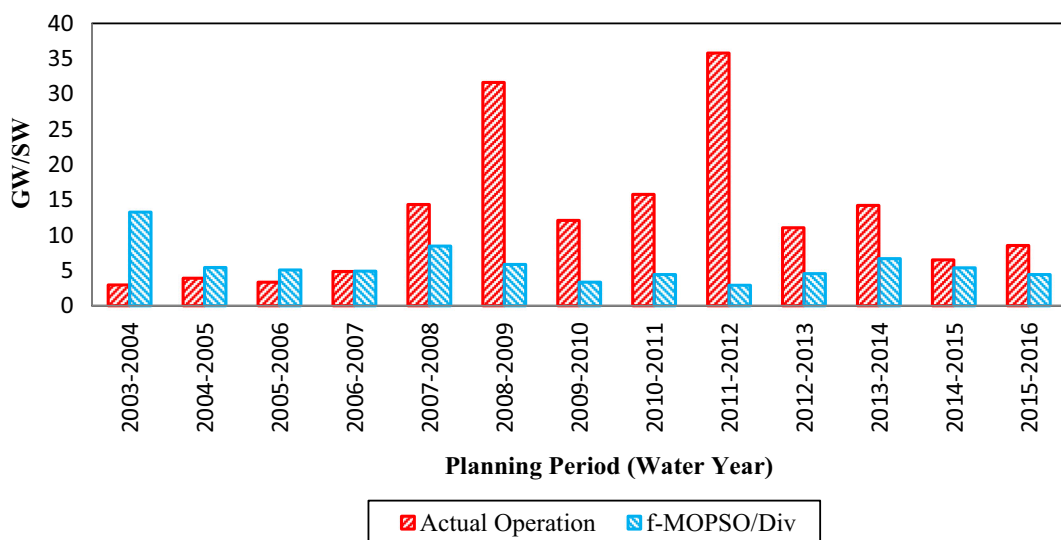

Fig. 13 Ratio of the groundwater extraction to the surface water allocation in the Nekouabad-Right region
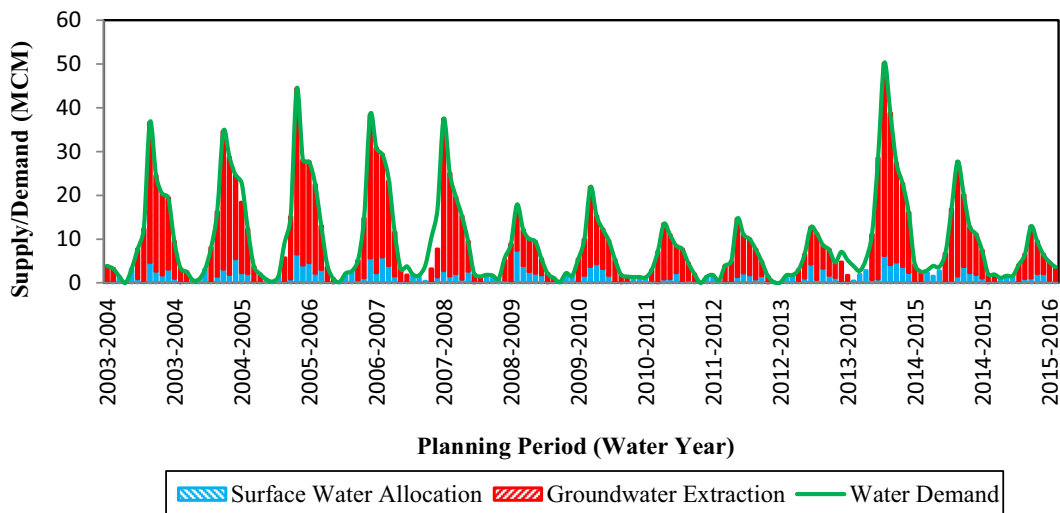
Fig. 14 Surface water and groundwater allocated to the Nekouabad-Left region and the water demands

operation. While in 2003–2004 water year, the GWL is raised by 2.76 m, in 2004–2005 the GWL withdraws by − 1.44 m, mainly due to the low precipitation and also the low recharge by the river in this water year. The occurrence of a drought condition in 2007–2008 water year poses very low precipitation and also low surface water allocation to the region resulting in − 0.92-m drawdown this year. Meanwhile, the demand percentage met and also the water productivity both decline by 25% and 50%, respectively, illustrating an acute condition for water resources management in this year. In 2012–2013, due to the proper recharge of the aquifer and considering low water demands for the main crops

in the region, the GWL was raised by 3.82 m as the highest rise in the GWL over the whole 13-year period.

In conclusion, in the Nekouabad-Left region, the water demands are averagely met by 94.4%, and the GWL is raised by 1.46 m, while the GWL withdraws by − 21.98 m in the actual operation of the region. Furthermore, the average water productivity is obtained to be 0.916 kg/m^3, which is larger than 0.841 kg/m^3 reported in the basin. It is noteworthy that the irrigation efficiency in both study sub-areas is computed above 74%, which is significantly higher than that in the actual operation in the basin, which is estimated to be 58%.
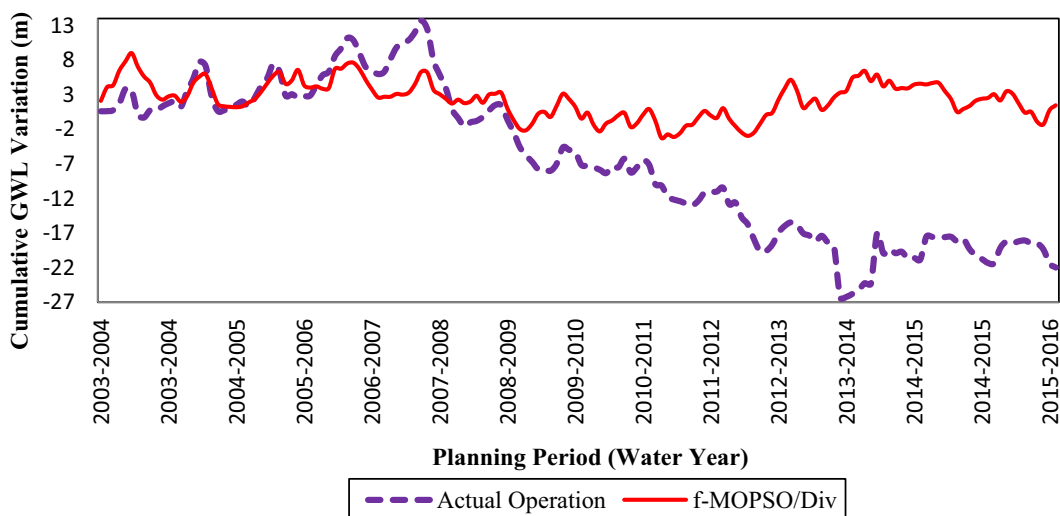

Fig. 15 Cumulative groundwater level variation in the Nekouabad-Left region

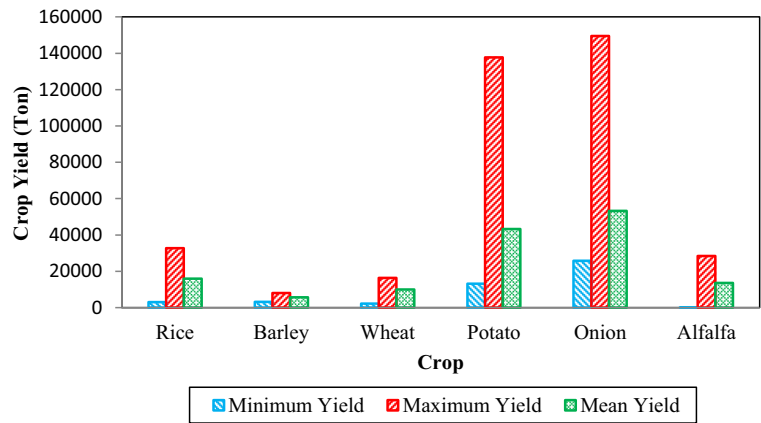**Fig. 16** Crop yield for the dominant crops over the whole planning period for the Nekouabad-Left region

Figure 14 shows the volume of the water supply and demands. Figure 15 depicts the cumulative GWL drawdown modeled versus that in the actual operation. Figure 16 displays a statistical chart presenting the six main crop yields, and finally, Fig. 17 illustrates the ratio of the groundwater extraction to the surface water allocation compared to the actual operation, all in the Nekouabad-Left region.

Conclusion

In this paper, an improved multi-objective particle swarm optimization algorithm named f-MOPSO/Div was proposed as an improved version of our recently proposed f-MOPSO algorithm. While the f-MOPSO deals with the multi-objective nature of the optimization problems using a comprehensive dominance index (DI) to choose the *Pbest* and the *Gbest* particles, the f-MOPSO/Div can benefit from the DI only when assigning the *Pbests* to the particles. Then, it selects the non-dominated *Pbest* that is located in the least-densely populated region in the objective space as the *Gbest* of the swarm at each iteration.

To better handle the high-dimensional problems, we recommended incorporating a polynomial mutation with an adaptive dynamic mutation probability into the f-MOPSO/Div.

In f-MOPSO, there is a pre-optimization process before the main optimization process. This pre-optimization process can be a very time-consuming and also an imprecise process, especially when dealing with large-scale multi-objective optimization problems. Hence, in the proposed f-MOPSO/Div, the pre-
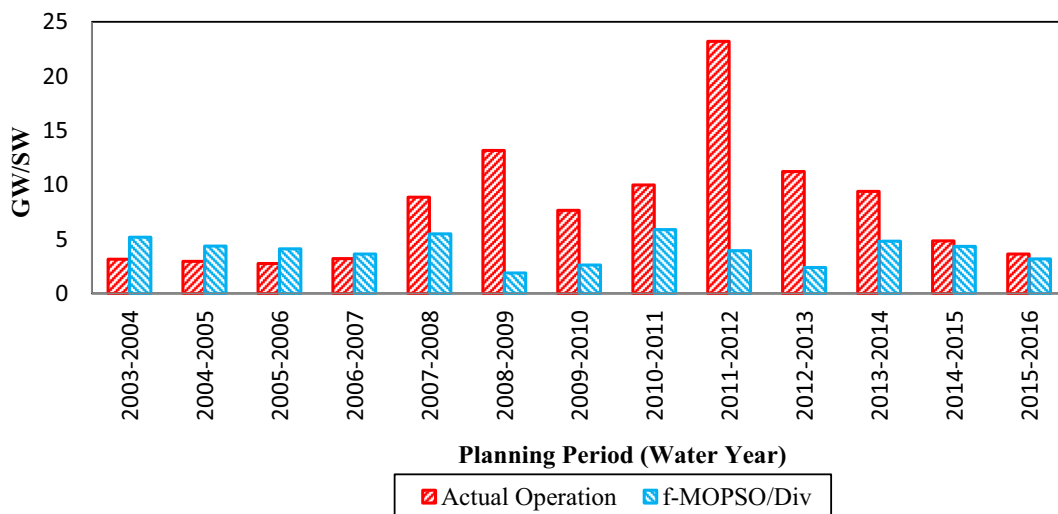
Fig. 17 Ratio of the groundwater extraction to the surface water allocation in the Nekouabad-Left region

optimization process is removed and incorporated into the main structure of the algorithm.

To validate the f-MOPSO/Div, it was applied to 14 well-known low- and high-dimensional multi-objective test problem suites and compared to two popular multi-objective evolutionary optimization algorithms as well as the original f-MOPSO. After the superiority of the proposal was revealed, this algorithm was applied to a practical engineering optimal conjunctive water use problem to benchmark the capabilities of f-MOPSO/Div to deal with real-world problems. Overall, the method can hold a suitable balance between recharging and discharging factors of the groundwater reservoir, such that the cumulative groundwater level drawdowns can be much reduced over the whole planning period as compared to what is seen in the actual operation. Water productivity and irrigation efficiency are among other factors ameliorated by the proposed model.

In the future works, we aimed at examining other objectives that could be addressed in the conjunctive water use problems. Taking uncertainty into account both in the simulation and optimization models could be another field of interest to be addressed in the future to reflect the uncertain nature of the conjunctive water use problems, mainly resulting from climate change in the study areas.

Compliance with ethical standards

Conflict of interest The authors declare that there are no conflicts of interest.

References

Abido, M. A. (2010). Multiobjective particle swarm optimization with nondominated local and global sets. *Natural Computing, 9*, 747–766.

Afshar, A., Zahraei, A., & Marino, M. A. (2010). Large-scale nonlinear conjunctive use optimization problem: decomposition algorithm. *Journal of Water Resources Planning and Management, ASCE, 136*(1), 59–71.

Agrawal, S., Dashora, Y., Tiwari, M., & Son, Y.–. J. (2008). Interactive particle swarm: a Pareto-adaptive metaheuristic to multiobjective optimization. *IEEE Transactions on Systems, Man, and Cybernetics Part A: Systems and Humans, 38*, 258–277.

Balling, R., & Wilson, S. (2001). The maxi-min fitness function for multiobjective evolutionary computation: application to city planning, In: *Proceedings of the Genetic and Evolutionary Computation Conference (GECCO'2001)*, pp. 1079–1084.

Ben Said, L., Bechikh, S., & Ghedira, K. (2010). The r-dominance: a new dominance relation for interactive evolutionary multicriteria decision making. *IEEE Transactions on Evolutionary Computation, 14*, 801–818.

Burt, O. R. (1964). The economics of conjunctive use of ground and surface water. *Hilgardia., 36*(2), 25–41.

Deb, K., & Deb, D. (2014). Analyzing mutation schemes for real-parameter genetic algorithms. *International Journal of Artificial Intelligence and Soft Computing, 4*(1), 1–28.

Deb, K., Pratap, A., Agarwal, S., & Meyarivan, T. (2002). A fast and elitist multiobjective genetic algorithm: NSGA-II. *IEEE Transactions on Evolutionary Computation, 6*(2), 182–197.

Drechsler, N., Drechsler, R., & Becker, B. (2001). Multi-objective optimization based on relation favour. In *Evolutionary multicriterion optimization* (pp. 154–166). Berlin: Springer.

Durillo, J. J., García-Nieto, J., Nebro, A. J., Coello, C. A. C., Luna, F., & Alba, E. (2009). Multi-objective particle swarm optimizers: An Experimental Comparison. In: Ehrgott M., Fonseca C.M., Gandibleux X., Hao JK., Sevaux M. (eds) *Evolutionary Multi-Criterion Optimization. EMO 2009. Lecture Notes in Computer Science,* vol 5467. Springer, Berlin, Heidelberg. https://doi.org/10.1007/978-3-642-01020-0_39.

Garza-Fabre, M., Pulido, G. T., & Coello, C. A. C. (2009). Ranking methods for many-objective optimization, In: Aguirre A.H., Borja R.M., Garciá C.A.R. (eds) *MICAI 2009: Advances in Artificial Intelligence. MICAI 2009. Lecture Notes in Computer Science*. vol 5845. Springer, Berlin, Heidelberg. https://doi.org/10.1007/978-3-642-05258-3_56.

Goulart, F., & Campelo, F. (2016). Preference-guided evolutionary algorithms for many-objective optimization. *Information Sciences, 329*, 236–255.

Hollander, H. M., Mull, R., & Panda, S. N. (2009). A concept for managed aquifer recharge using ASR-wells for sustainable use of groundwater resources in an alluvial coastal aquifer in Eastern India. *Physics and Chemistry of the Earth, 34*, 270–278.

Ireland, D., Lewis, A., Mostaghim, S., & Lu, J. W. (2006). Hybrid particle guide selection methods in multi-objective particle swarm optimization, In *Proceedings of the second IEEE international, Conference on e-science and grid computing 2006,* (e-Science'06).

Jahandideh-Tehrani, M., Bozorg-Haddad, O., & Loáiciga, H. A. (2020). Application of particle swarm optimization to water management: an introduction and overview. *Environmental Monitoring and Assessment, 192*, 281.

Kaur, R., Paul, M., & Malik, R. (2007). Impact assessment and recommendation of alternative conjunctive water use strategies for salt affected agricultural lands through a field scale decision support system- A case study. *Environmental Monitoring and Assessment, 129*, 257–270.

Kennedy, J., & Eberhart, R. (1995). Particle swarm optimization, In *Proc International Conference on Neural Networks,* Perth, Australia, IEEE Piscataway NJ, pp. 1942-1948.

Laumanns, M., Thiele, L., Deb, K., & Zitzler, E. (2002). Combining convergence and diversity in evolutionary multiobjective optimization. *Evolutionary Computation, 10*, 263–282.

Li, L., Wang, W., & Xu, X. (2017). Multi-objective particle swarm optimization based on global margin ranking. *Information Sciences, 375*, 30–47.

Lin, Q., Li, J., Du, Z., Chen, J., & Ming, Z. (2015). A novel multi-objective particle swarm optimization with multiple search strategies. *European Journal of Operational Research, 247*(3), 732–744.

Liu, Y., Gong, D., Sun, X., & Zhang, Y. (2017). Many-objective evolutionary optimization based on reference points. *Applied Soft Computing, 50*, 344–355.

Liu, J., Zhang, H., He, K., & Jiang, S. (2018). Multi-objective particle swarm optimization algorithm based on objective space division for the unequal-area facility layout problem. *Expert Systems with Applications, 102*, 179–192.

McPhee, J., & Yeh, W. W.-G. (2004). Multi objective optimization for sustainable groundwater management in semiarid regions. *J Water Res Plan Manage, ASCE, 130*(6), 490–497.

Mostaghim, S., & Teich, J. (2003a). Strategies for finding good local guides in multi-objective particle swarm optimization (MOPSO). In *IEEE Swarm Intelligence Symposium. IIN April IEEE Service Center Piscataway* NJ, pp. 26-33.

Mostaghim, S., & Teich, J. (2003b). The role of ε-dominance in multiobjective particle swarm optimization methods., In *Proceedings of IEEE congress on evolutionary computation CEC'2003,* Canberra, Australia pp. 1764-1771.

Nebro, A., Durillo, J. J., Garcia-Nieto, J., Barba-Gonzalez, C., Del Ser, J., Coello, C. A. C., Benitez-Hidalgo, A., & Aldana-Montes, J. F. (2018). Extending the speed-constrained multi-objective PSO (SMPSO) with reference point base preference articulation. International Conference on Parallel problem Solving from Nature, Springer, Cham, 298-310.

Peralta, R. C., Forghani, A., & Fayad, H. (2014). Multiobjective genetic algorithm conjunctive use optimization for production, cost and energy with dynamic return flow. *J Hydrol, 511*, 776–785.

Qu, B., Li, C., Liang, J., Yan, L., Yu, K., & Zhu, Y. (2020). A self-organized speciation based multi-objective particle swarm optimizer for multimodal multi-objective problems. *Applied Soft Computing Journal, 86*, 105886. https://doi.org/10.1016/j.asoc.2019.105886.

Rezaei, F., Safavi, H. R., Mirchi, A., & Madani, K. (2017a). f-MOPSO: an alternative multi-objective PSO algorithm for conjunctive water use management. *Journal of Hydro-environment Research, 14*, 1–18.

Rezaei, F., Safavi, H. R., & Zekri, M. (2017b). A hybrid fuzzy-based multi-objective PSO algorithm for conjunctive water use and optimal multi-crop pattern planning. *Water Resources Management, 31*(4), 1139–1155.

Safavi, H. R., & Rezaei, F. (2015). Conjunctive use of surface and ground water using fuzzy neural network and genetic algorithm. *IJSTC, 39*(C2), 365–377.

Safavi, H. R., Darzi, F., & Marino, M. A. (2010). Simulation-optimization modeling of conjunctive use of surface water and groundwater. *Water Resour Manage, 24*, 1965–1988.

Sahoo, N. C., Ganguly, S., & Das, D. (2011). Simple heuristics-based selection of guides for multi-objective PSO with an application to electrical distribution system planning. *Engineering Applications of Artificial Intelligence, 24*, 567–585.

Sierra, M. R., & Coello, C. A. C. (2005). Improving PSO-based multi-objective optimization using crowding, mutation and ε-dominance. In *Proceedings of Evolutionary Multi-Criterion Optimization.*

Srivastava, P., & Singh, R. M. (2017). Agricultural land allocation for crop planning in a canal command area using fuzzy multiobjective goal programming. *Journal of Irrigation and Drainage Engineering, 143*, 04017007. https://doi.org/10.1061/(ASCE)IR.1943-4774.0001175.

Sun, Q., Xu, G., Ma, C., & Chen, L. (2017). Optimal crop-planting area considering the agricultural drought degree. *Journal of Irrigation and Drainage Engineering, 143*, 04017050. https://doi.org/10.1061/(ASCE)IR.1943-4774.0001245.

Tayebikhorami, S., Nikoo, M. R., & Sadegh, M. (2019). A fuzzy multi-objective optimization approach for treated wastewater allocation. *Environmental Monitoring and Assessment, 191*, 468.

Thiele, L., Miettinen, K., Korhonen, P. J., & Molina, J. (2009). A preference-based evolutionary algorithm for multi-objective optimization. *Evolutionary Computation, 17*, 411–436.

Wang, R., Xiong, J., Ishibuchi, H., Wu, G., & Zhang, T. (2017). On the effect of reference point in MOEA/D for multi-objective optimization. *Applied Soft Computing, 58*, 25–34.

Wong, Y. J., Arumugasamy, S. K., Chung, C. H., Selvarajoo, A., & Sethu, V. (2020). Comparative study of artificial neural network (ANN), adaptive neuro-fuzzy inference system (ANFIS) and multiple linear regression (MLR) for modeling of Cu (II) adsorption from aqueous solution using biochar derived from rambutan (Nephelium lappaceum) peel. *Environmental Monitoring and Assessment, 192*, 439.

Yadav, R. K., Kumar, A., Lal, D., & Batra, L. (2004). Yield responses of winter (Rabi) forage crops to irrigation with saline drainage water. *Experimental Agriculture, 40*, 65–75.

Yang, J., Zhou, J., Liu, L., & Li, Y. (2009a). A novel strategy of pareto-optimal solution searching in multi-objective particle swarm optimization (MOPSO). *Computers and Mathematics with Applications, 57*, 1995–2000.

Yang, C. C., Chang, L. C., Chen, C. S., & Yeh, M. S. (2009b). Multi-objective planning for conjunctive use of surface and subsurface water using genetic algorithm and dynamics programming. *Water Resour Manage, 23*, 417–437.

Yang, S., Li, M., Liu, X., & Zheng, J. (2013). A grid-based evolutionary algorithm for many-objective optimization. *IEEE Transactions on Evolutionary Computation, 17*, 721–736.

Yekom Consulting Engineers (2013). *Studies for updating Iran's integrated water plan (Gavkhouni River Basin),* Final report, Water and Wastewater section, Ministry of Energy (In Persian).

Yeom, J.-M., Lee, C.-S., Park, S.-J., Ryu, J.-H., Kim, J.-J., Kim, H.-C., & Han, K.-S. (2015). Evapotranspiration in Korea estimated by application of a neural network to satellite images. *Remote Sensing Letters, 6*(6), 429–438.

Yousefi, M., Banihabib, M. E., Soltani, J., & Roozbahani, A. (2018). Multi-objective particle swarm optimization model

for conjuctive use of treated wastewater and groundwater. *Agricultural Water Management, 208*, 224–231.

Zayandab Consulting Engineers (2008). *Studies of water supplies and demands in the Zayandeh-Rud River Basin, The Preliminary Studies,* 5th Volume, Agricultural Studies (In Persian).

Zeinali, M., Azari, A., & Heidari, M. M. (2020). Multiobjective optimization for water resource management in low-flow areas based on a coupled surface water–groundwater model. *J. Water Resour. Plann. Manage., 146*(5), 04020020.

Zeleny, M. (1973). Compromise programming, multiple criteria decision-making. In J. L. Cochrane & M. Zeleny (Eds.), *Multiple criteria decision making* (pp. 263–301). Columbia: University of South Carolina Press.

Zhou, A., Zhao, S., Suganthan, P. N., Liu, W., & Tiwari, S. (2009). Multiobjective optimization test instances for the CEC 2009 special session and competition. In *Proceedings of University of Essex, Colchester, UK and Nanyang Technological University, Singapore, Special Session on Performance Assessment of Multi-Objective Optimization Algorithms,* Technical Report (2008).